Chapter 5

Results & Discussion:

(Water absorption, mechanical and tribological properties of natural fiber reinforced composites)

Water absorption, mechanical and tribological properties of natural fiber reinforced epoxy composites

5.1 Water absorption properties of the NFRECs

Natural fibers has a tendency to absorb more moisture from the air when compared to man made fibers like aramid fibers, carbon fibers etc. This property of the natural fibers contribute to its poor fiber-matrix adhesion. Also, because water absorption is a major issue for bio-composites' outdoor applications, this present research will focus on the water retention characteristics of NFRECs.

5.1.1 Influence of chemical treatment on water absorption properties of HFREC

Fig. 5.1 shows the percentage of water absorbed by UT, ST, and PT HFREC from a time interval of 24–192 h. All the tested composite specimens (both UT and treated fiber composites) were reinforced with the same percentage (19%) of fiber loading, therefore similar trends in water resistance were observed for all the composites.[62] From Fig. 4, it can be seen that there is a sharp increase in water absorption rate up to 120 h for both UT and treated HFREC. After 120 h, the water absorption rate reduces and remains constant for all the composite specimens due to the saturation limit of the composite specimens. Similar experimental results were also confirmed by several researchers [99,100]. From Fig. 5.1, it can be seen that both the ST and PT HFREC showed higher resistance to water absorption in comparison with UT HFREC and PT HFREC exhibited the highest resistance to water absorption among all composites.

The elimination of hemicellulose and lignin during the chemical modification of hemp fibers seems to be accountable for the treated hemp fiber composites' reduced water absorption rate. In relation to water absorption, the hemicellulose in hemp fiber is more sensitive and accessible than the crystalline sections of cellulose [101]. Furthermore, chemical treatment may have improved the fiber–matrix interface bonding by minimizing the water molecule wicking at the interface and thereby increasing the water resistance of treated fiber composites [102,103].

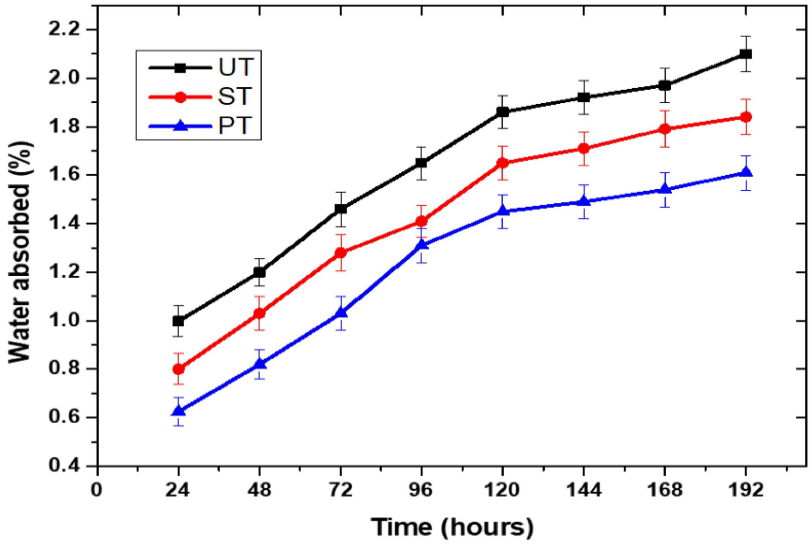

Figure 5.1 Percentage of water absorbed by untreated (UT), sodium carbonate treated (ST), and peroxide treated (PT) hemp fiber reinforced epoxy composites

5.1.2 Effect of fiber coatings on water absorption properties of HFREC

Percentage of water absorbed by uncoated, PHB coated, and PLA coated HFREC were displayed in Fig. 5.2. From the Fig. 5.2, it was observed that initially all the HFREC samples, both in case of uncoated and coated fibers, absorb water quickly (upto 120 h) but once the saturation is achieved, the rate of water absorption becomes almost constant. Several researchers also confirmed similar observations [100,101].

From the Fig. 5.2, it is also observed that the composites reinforced with PHB and PLA coated fibers had better resistance to water absorption in comparison to uncoated hemp fiber composites and the best resistance to water absorption was shown by PLA coated HFREC. This can be due to the polymer coating of the fiber which may have reduced the hydrophilic nature of the fibers and have enhanced the fiber-matrix bonding [102,103].

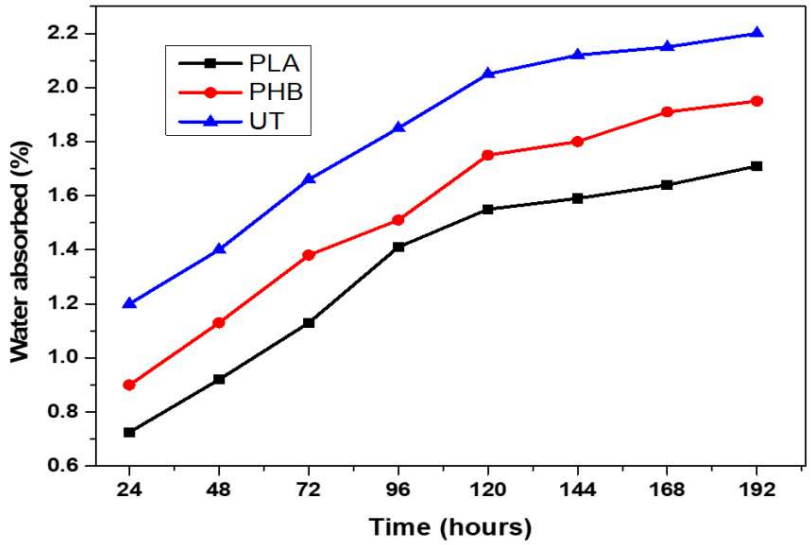

Figure 5.2. Percentage of water absorbed by untreated HFREC, PHB coated HFREC, and PLA coated HFREC.

5.1.3 Influence of glutamic acid treatment on the moisture retention properties of SFREC

The water assimilation rate of untreated (UT) SFREC, alkali treated (AT) SFREC, glutamic acid treated (GT) SFREC and combination of alkali and glutamic acid treated (AGT) SFREC were represented in Fig. 5.3. (upto 120 h). From Fig. 5.3, it can be observed that the chemical modification of the sisal fibers had significantly reduced the water absorption rate of the chemically treated SFREC. The highest

apparent porosity value was obtained for the untreated SFREC and the least water absorption rate was obtained for AGT SFREC among the chemically treated composites, It was due to the rough surface of the chemically modified sisal fibers forming a mechanical interlocking with the polymer matrix, which primarily contributed to the enhanced interface bonding [100,103]. Because more matrix materials were drawn to the rough sisal fiber surface, the combination of the chemically treated fibers and the polymer matrix materials were dense, resulting in a decreased water retention rate of the chemically treated SFREC [102].

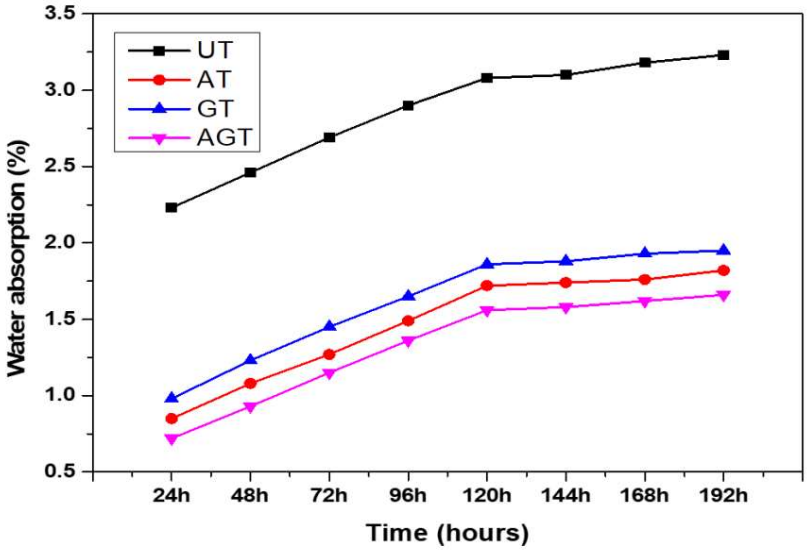

Figure 5.3 Water absorption (%) of untreated (UT), alkali (AT), gluatmic acid (GT) and combination of alkali and glutamic acid (AGT) treated SFREC.

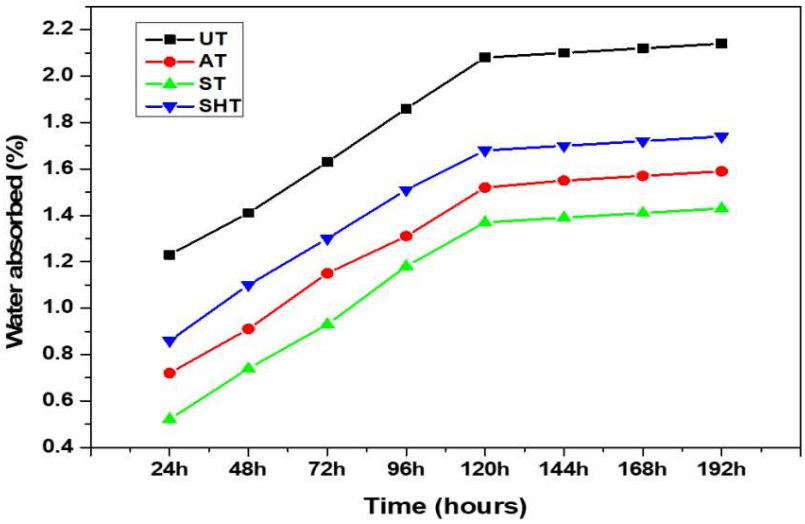

Figure 5.4 Percentage of water absorbed by UT JFREC, AT JFREC, ST JFREC and SHT JFREC.

5.1.4 Influence of chemical treatment on water absorption characteristics of JFREC

Water absorption characteristics of raw and modified JFREC specimens are represented in Figure 5.4. From the Fig. 5.4, it is evident that up to 120 h the water assimilation rate of un-modified and modified JFREC is high but after 120 h when the saturation point is reached, the rate of water absorption becomes almost constant for both treated and untreated JFREC. Similar findings are also observed by several researchers [99,100]. From the Fig. 5.4, it can be seen that the percentage of water assimilation of untreated JFREC is higher in comparison to chemically modified JFREC. This is because the chemical modification has reduced the polarity of the jute fiber inducing appreciable interfacial adhesion between hydrophilic jute and hydrophobic epoxy [101-103]. Comparing the water retention properties of all the JFREC, the best water accumulation behavior was shown by SCT JFREC.

5.2 Mechanical properties of natural fiber reinforced epoxy composites

It is important to understand any natural fiber composites' suitability for a certain application before choosing it, and this can be done by understanding about its tensile, impact, interlaminar shear strength, flexural and micro-hardness properties. Mechanical behaviour of these NFRECs primarily depends on fiber-matrix interfacial adhesion [40,41]. This research will focus on the the influence of various chemical treatment on the fiber surface and fiber coating on the mechanical aspects of NFRECs.

5.2.1 Influence of chemical treatment on tensile properties of HFREC

The tensile stress–strain curves of UT, ST, and PT HFREC are shown in Fig. 5.5 From Fig. 5.5, it can be observed that the PT and UT HFREC exhibited similar failure mode, whereas the ST HFREC exhibited comparatively lower failure mode. The lower failure mode observed in ST HFREC may be due to the efficient stress transfer between the fiber and the matrix resulting from improved mechanical interlocking between the treated fiber and the epoxy matrix [62]. The variations in tensile strength and modulus of HFREC due to sodium carbonate and peroxide treatment of the fiber are displayed in Fig. 5.6(A) and Figure 5.6(B). Both the tensile strength and tensile modulus of HFREC have considerably improved due to chemical modification as shown in Fig. 5.6(A,B). ST and PT HFREC showed an enhancement of 16.9% and 29.3% in tensile strength and 6.2% and 18.7% in tensile modulus over UT HFREC. Several researchers have mentioned similar results in their investigations [99,104, 105]. Fibrillation of fibers, increase in roughness of fiber surface, and lowering of hydrophilic nature of hemp fiber caused by both sodium carbonate and peroxide

treatment of the fiber contributed to the better mechanical interlocking between hemp fiber and epoxy resin resulting in improvement of tensile properties of treated HFREC [64].

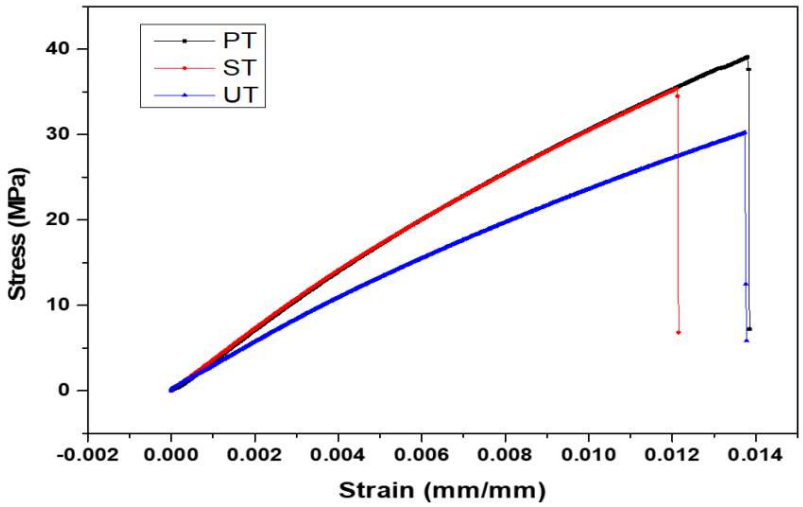

Figure 5.5 Stress–strain curves of UT HFREC, ST HFREC and PT HFREC.

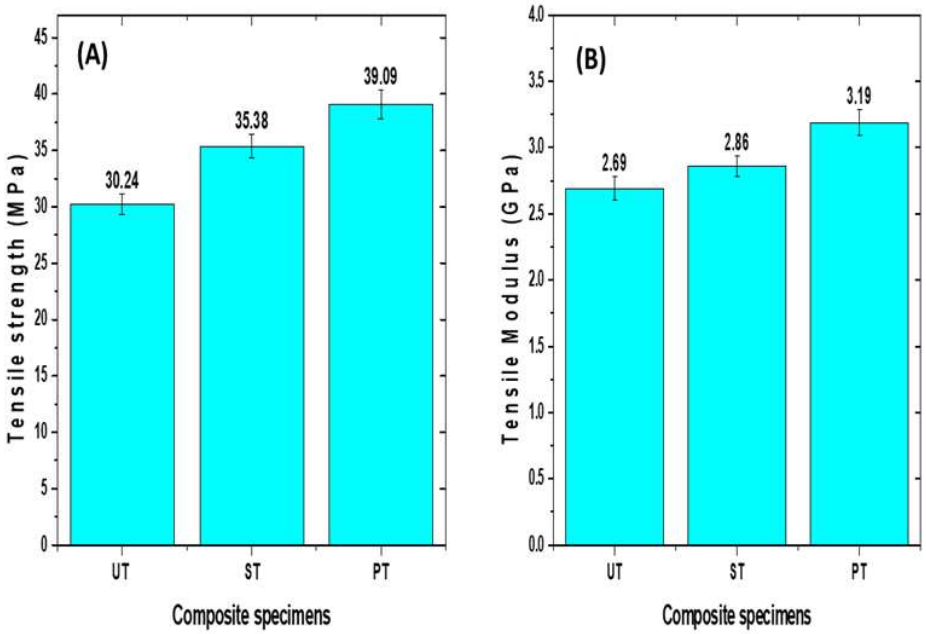

Figure 5.6 Tensile properties of hemp fiber reinforced epoxy composites (HFREC): (A) Tensile strength of UT HFREC, ST HFREC and PT HFREC. (B) Tensile modulus of UT HFREC, ST HFREC and PT HFREC.

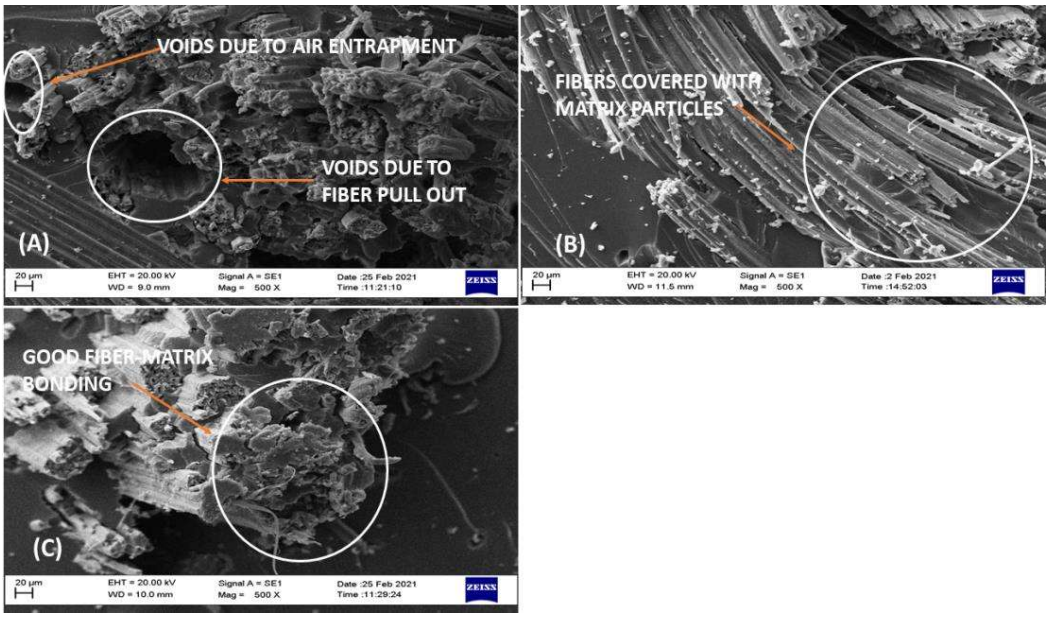

Figure 5.7 Scanning electron microscopy images of tensile fractured surfaces of hemp fiber reinforced epoxy composites (HFREC) at 500X: (A) untreated HFREC, (B) sodium carbonate treated HFREC, and (C) peroxide treated HFREC

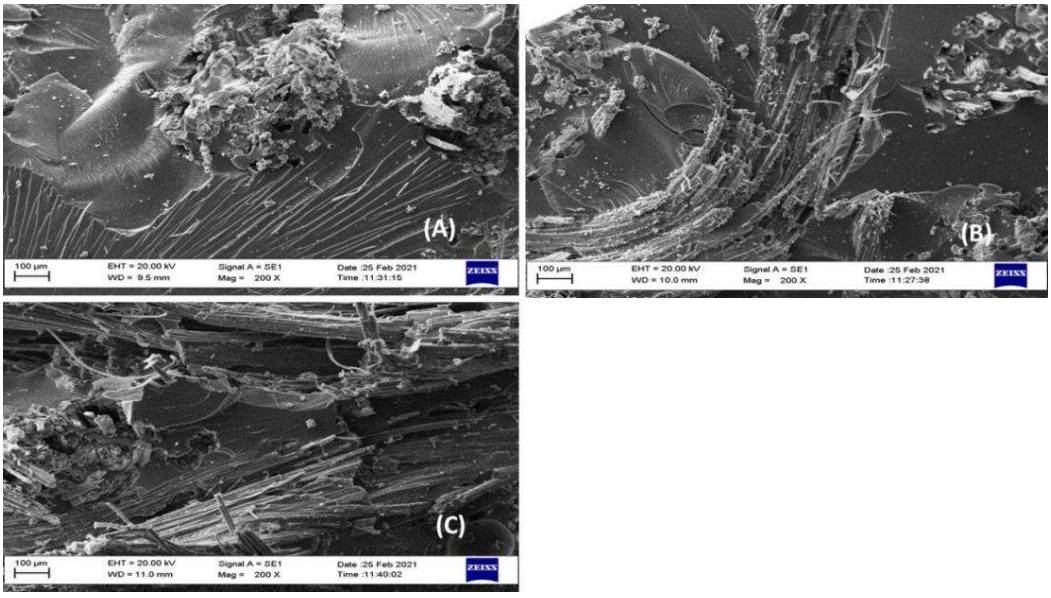

Figure 5.8 Scanning electron microscopy images of tensile fractured surfaces of hemp fiber reinforced epoxy composites (HFREC) at 200X: (A) untreated HFREC, (B) sodium carbonate treated HFREC, and (C) peroxide treated HFREC

5.2.1.1 SEM micrographs of tensile fractured surfaces of composites

Fig. 5.7 (at 500X) and Fig. 5.8 (at 200X) shows the SEM micrographs of tensile fractured surfaces of UT, ST, and PT HFREC. The presence of voids due to air entrapment can be found in the fractured surface of UT HFREC in Fig. 5.7(A). Additional holes or voids due to the fiber pullout can also be observed on the UT HFREC fractured surface contributing to its poor mechanical strength as a result of inefficient stress transfer. However, the SEM images of the tensile fractured surface of ST HFREC and PT HFREC show that the matrix particles have still adhered to the fibers even after the fracture (Fig. 5.7(B,C)). This signifies that both the chemical treatment (sodium carbonate and peroxide) have enhanced the mechanical interlocking between the fiber and the matrix, which may have resulted in the improvement of their mechanical properties [106,107]. This improvement in mechanical properties was more dominant in the case of PT HFREC, which can be confirmed by the SEM image of its fractured surface where a lesser number of void and good fiber–matrix bonding can be observed.

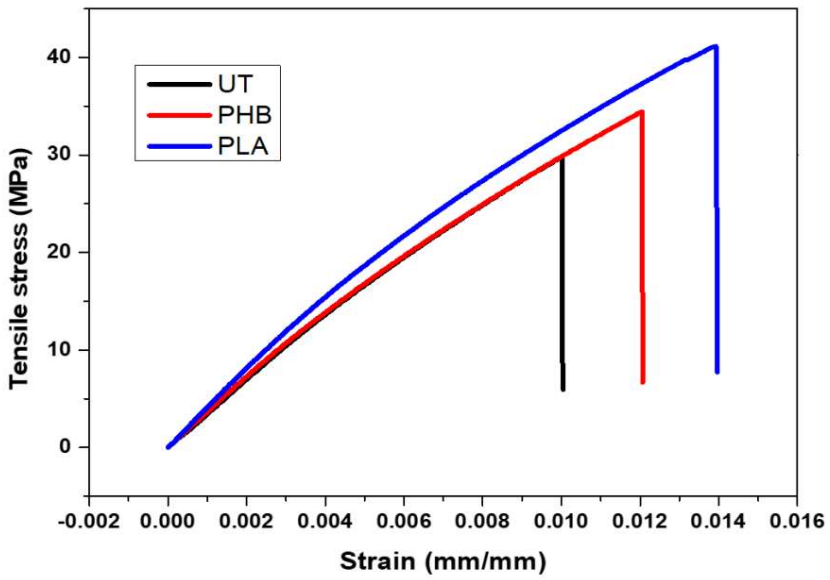

Figure 5.9 Stress–strain curves of UT HFREC, PHB coated HFREC and PLA coated HFREC.

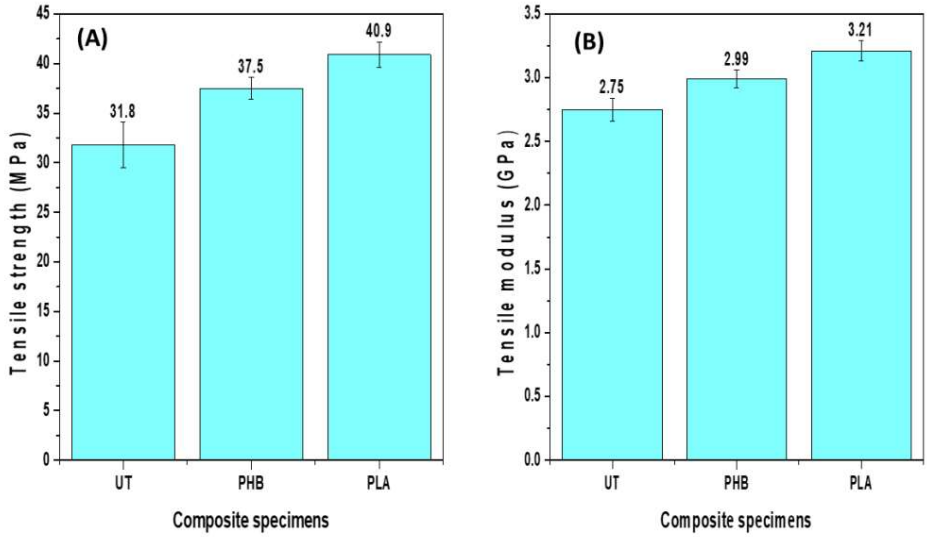

Figure 5.10 Tensile properties of hemp fiber reinforced epoxy composites (HFREC): (A) Tensile strength of UT HFREC, PHB coated HFREC and PLA coated HFREC. (B) Tensile modulus of UT HFREC, PHB coated HFREC and PLA coated HFREC.

5.2.2 Effect of fiber coatings on tensile properties of HFREC

The tensile stress–strain curves obtained from the tensile tests of uncoated HFREC, PHB coated HFREC, and PLA coated HFREC are shown in Fig. 5.9. The tensile strength and tensile modulus of uncoated, PHB coated, and PLA coated HFREC are shown in Fig. 5.10(A) and Fig. 5.10(B). From the Fig. 5.10(A) and Fig. 5.10(B), it is evident that the polymer coating of fiber surface has led to an improvement in both tensile strength and tensile modulus of the composites. PHB coated HFREC and PLA coated HFREC showed an improvement of 17.9% and 28.6% in tensile strength and 8.7% and 16.7% in tensile modulus over composites reinforced with uncoated hemp fibers. Fibrillation of fibers caused by sodium hydrogen carbonate treatment and the ability of both PHB and PLA surface coating to change the hydrophilic nature of the fiber to hydrophobic nature may have resulted in improved mechanical interlocking between the fiber and the polymer matrix which in turn improved the tensile

properties of the coated HFREC. Similar results were also observed in previous investigations [44,46,108].

5.2.2.1 Scanning electron microscopy analysis of tensile fracture surfaces

SEM analysis was done to observe the tensile fracture surfaces of uncoated, PHB coated, and PLA coated fiber composites and were shown in Fig. 5.11. Poor tensile strength of uncoated HFREC was due to the existence of voids which are clearly visible on its fractured surface Fig. 5.11(A). Some extra voids or holes due to the fiber pullout are also present on its fracture surface which may have resulted inadequate stress transfer. However, it can be observed from the SEM images of the tensile fracture surfaces of PHB coated HFREC and PLA coated HFREC that the epoxy matrix materials are still attached to the hemp fibers even after the tensile test (Fig. 5.11(B,C)). This is an indication of good fiber-matrix adhesion arising from both the polymer (PHB and PLA) coating of the fibers which may have resulted in improved tensile strength of coated fiber composites [45,46,107]. This enhancement in tensile strength was more prominent in case of PLA coated fiber composites which can also be verified from the SEM micrograph (Fig. 5.11(C)) of its fracture surface, where a small number of voids and improved fiber-matrix adhesion was visible.

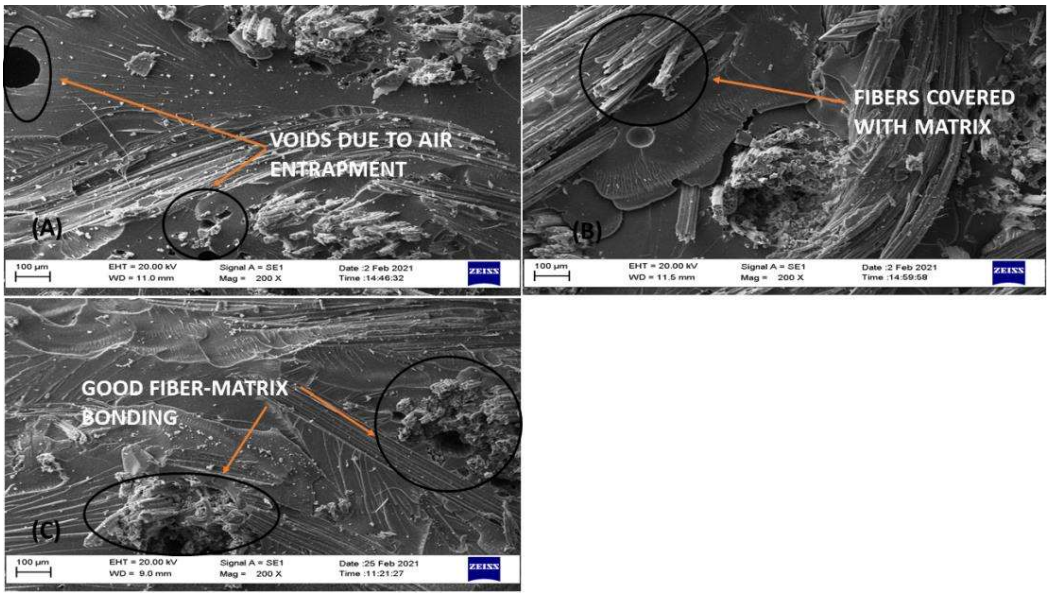

Figure 5.11 Scanning electron microscopy images of tensile fractured surfaces of hemp fiber reinforced epoxy composites (HFREC): (A) uncoated HFREC, (B) PHB coated HFREC, and (C) PLA coated HFREC.

5.2.3 Effect of chemical modification on tensile properties of SFREC

The effect of stearic acid and sodium citrate treatment on the tensile properties of SFREC were represented in Fig. 5.12(A,B). Due to the successful chemical surface modification, all treated SFREC composites exhibit greater tensile characteristics than those of untreated SFREC composites. Because of weak fibre–matrix bonding, the untreated SFREC has the lowest tensile characteristics. Stearic acid treated (SAT) SFREC has a 8.1% higher tensile strength and a 6.2% higher tensile modulus than untreated SFREC. The stearic acid treatment was able to eliminate the waxy material on the surface of fibers, resulting in enhanced surface roughness.This may be the explanation for the fibers' greater interfacial adhesion with the epoxy matrix [68]. Sodium citrate treated (SCT) SFREC has the highest tensile strength and tensile modulus among all sisal fiber composites, which are 23.3% and 16.9% greater than untreated SFREC, respectively. Sodium citrate treatment was responsible for the

removal of waxy substances along with partial elimination of hemicellulose and lignin from the fiber surface resulting in improvement of the surface roughness of the fiber. This may be the reason for strong interfacial adhesion of SCT SFREC among all the tensile tested SFREC [67]. The effect of sisal fiber surface treatment on the elongation at break of SFREC were shown in Fig. 5.13. The elongation at break of both the SAT and SCT modified composites was clearly greater than that of the untreated composite due to the improved fiber-matrix bonding between the surface treated sisal fiber and the epoxy. That is, the introduction of SAT and SCT fibers into the epoxy aided in the enhancement of the treated composites' ductile properties.

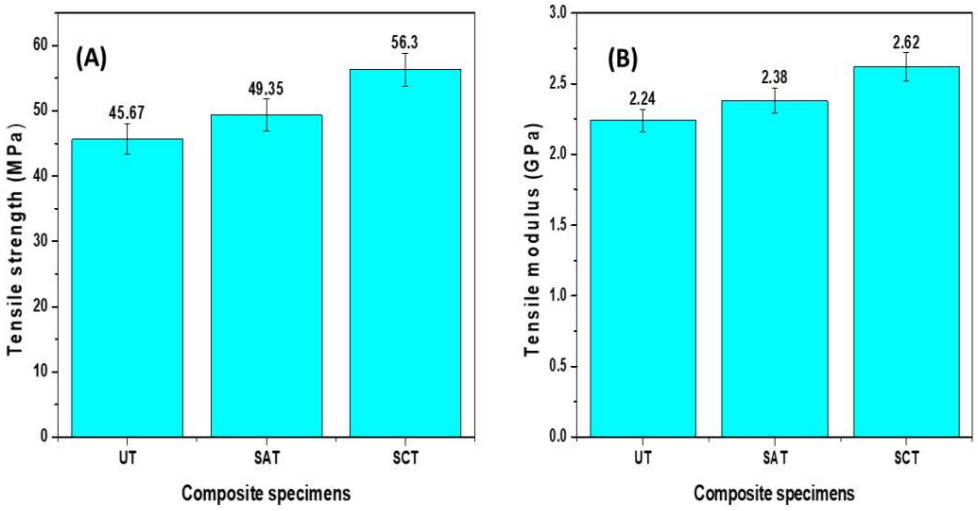

Figure 5.12 Tensile properties of sisal fiber reinforced epoxy composites (SFREC): (A) Tensile strength of UT SFREC, SAT SFREC and SCT SFREC. (B) Tensile modulus of UT SFREC, SAT SFREC and SCT SFREC

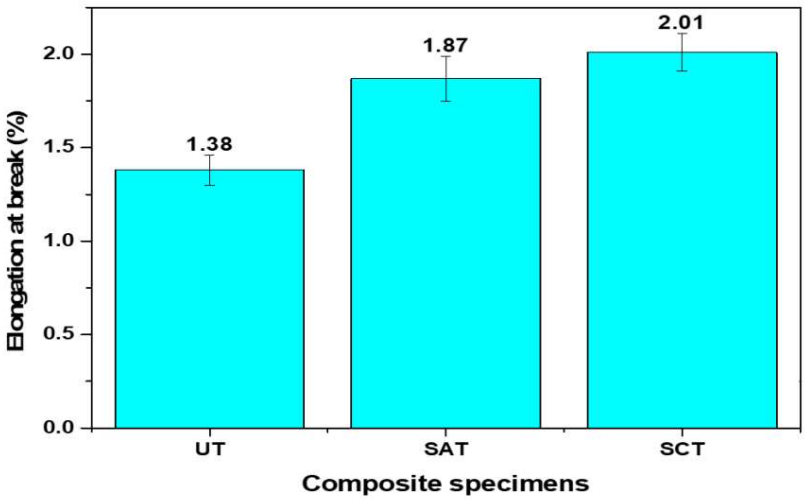

Figure 5.13 Elongation at break values (%) of UT SFREC, SAT SFREC and SCT SFREC

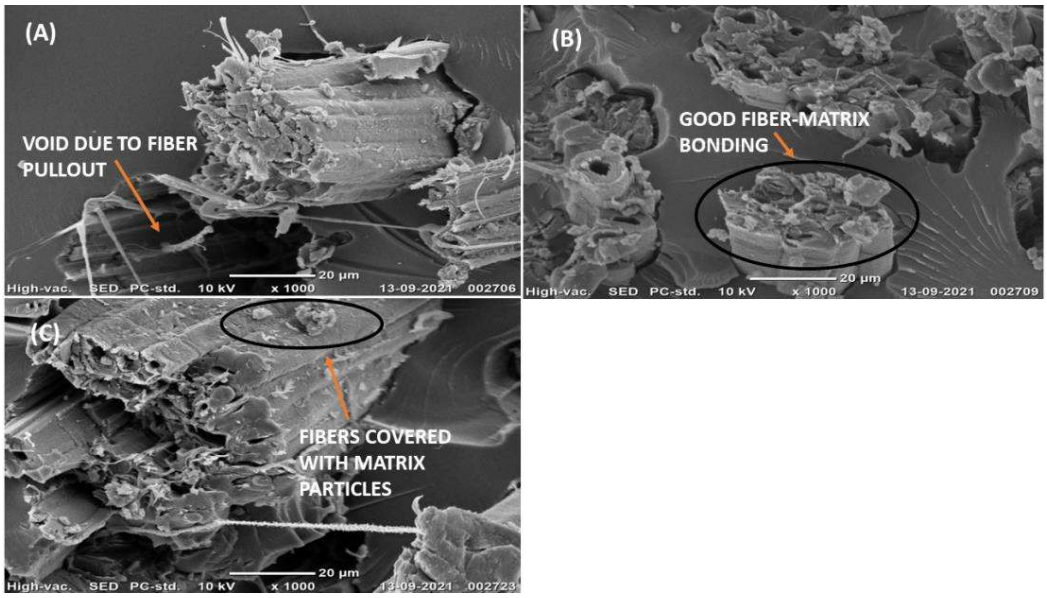

Figure 5.14 SEM images of tensile fractured surfaces of sisal fiber reinforced epoxy composites (SFREC) at 1000X: (A) untreated SFREC, (B) SAT SFREC, and (C) SCT SFREC

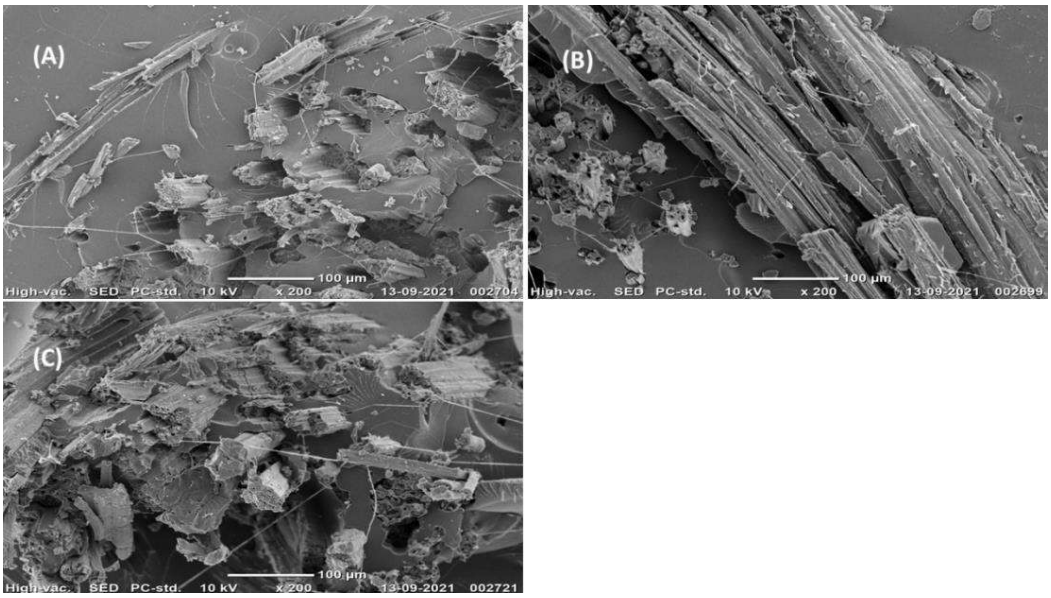

Figure 5.15 SEM images of tensile fractured surfaces of sisal fiber reinforced epoxy composites (SFREC) at 200X: (A) untreated SFREC, (B) SAT SFREC, and (C) SCT SFREC

5.2.3.1 Scanning electron microscopy analysis of tensile fracture surfaces

SEM micrographs of the specimen exposed to tensile stresses are shown in Fig. 5.14 (at 1000X) and Fig. 5.15 (at 200X). The fracture surface of untreated composites has pull-out fibres, as shown in Fig. 5.14(A), and the surfaces of pull-out sisal fibers appear to be smooth and clean. These results could imply a weak interfacial contact between the sisal fiber and the epoxy, and that the fibre-matrix interface is unable to properly transfer stress [106]. The SEM images of SAT SFREC (Fig. 5.14(B)) compared to untreated SFREC (Fig. 5.14(A)) show that the stearic acid treatment caused some modifications to the fracture surface. The sisal fibers were no longer pulled away from the epoxy matrix, indicating that the bond between the stearic acid treated sisal fiber and the epoxy matrix was good [107]. When compared to untreated and SCT SFREC, the fracture surface of the SAT SFREC composite had more flat fracture surfaces. The SEM image in Fig. 5.14(C) clearly shows that all fibers have

epoxy resin adhering to them after failure. The failing surface appears to be uniform in appearance. This indicates that the treated fibre and epoxy matrix have a greater interfacial contact.

5.2.4 Influence of chemical treatment on tensile properties of JFREC

Fig. 5.16 shows the tensile stress-strain curves of untreated, sodium hydroxide, sodium carbonate and sodium hydrogen carbonate treated JFREC. It can be observed from the Fig. 5.16 that the NaOH treated (AT) JFREC and $NaHCO_3$ treated (SHT) JFREC showed similar failure behavior, the untreated JFREC exhibited relatively lower failure mode and the Na_2CO_3 treated (ST) JFREC showed the longer failure mode among all the tensile tested composites.

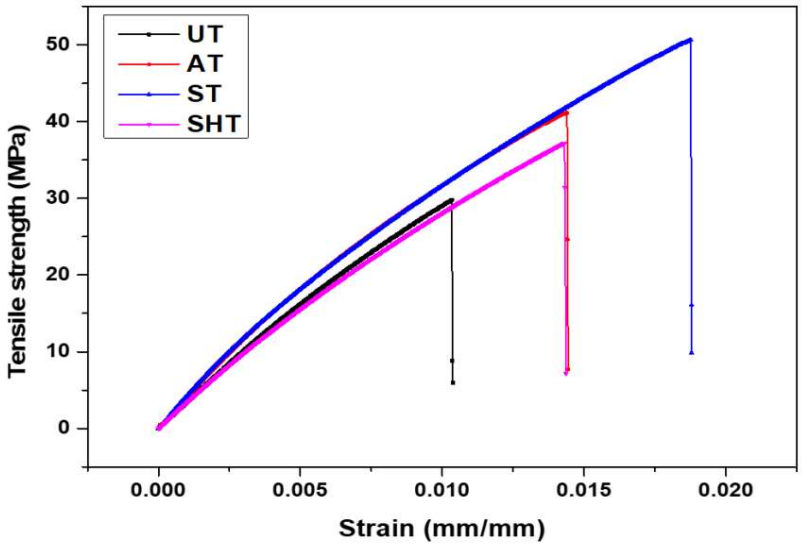

Figure 5.16 Stress–strain curves of UT JFREC, AT JFREC, ST JFREC and SHT JFREC.

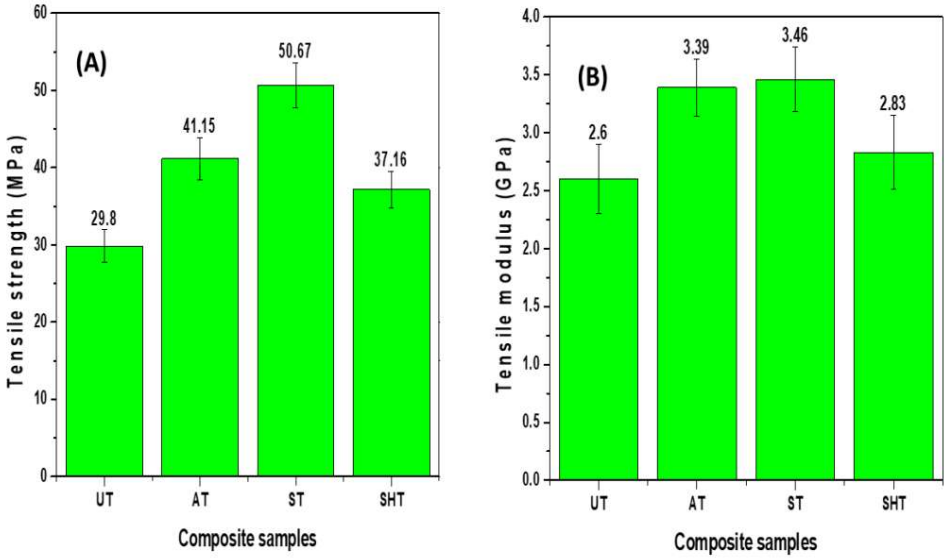

Figure 5.17 Tensile properties of jute fiber reinforced epoxy composites (JFREC): (A) Tensile strength of UT JFREC, AT JFREC, ST JFREC and SHT JFREC. (B) Tensile modulus of UT JFREC, AT JFREC, ST JFREC and SHT JFREC.

Fig. 5.17(A) and Fig. 5.17(B) represents the influence of various surface treatments on the tensile strength and tensile modulus of the JFREC. It is apparent from both the Fig. 5.17(A) and Fig. 5.17(B) that, owing to the chemical alteration of the outer layer of the fiber, the tensile strength and modulus of the JFREC is greatly improved. Relative to untreated fiber composite, there is an improvement of 38.1%, 70.1%, and 24.7% in tensile strength and 30.6%, 33.1%, and 8.9% in tensile modulus for composites prepared with sodium hydroxide, sodium carbonate, and sodium hydrogen carbonate treated fibers respectively. Similar results were also observed in previous studies [86,109]. This enhancement in tensile properties of treated JFREC in comparison to untreated JFREC is attributable to the rough fiber surface and also because of the fibrillation of the fiber which enhances fiber-matrix interlocking. The

reduction in the hydrophilic quality of jute fibers by chemical modification is another cause for this improvement in properties [110].

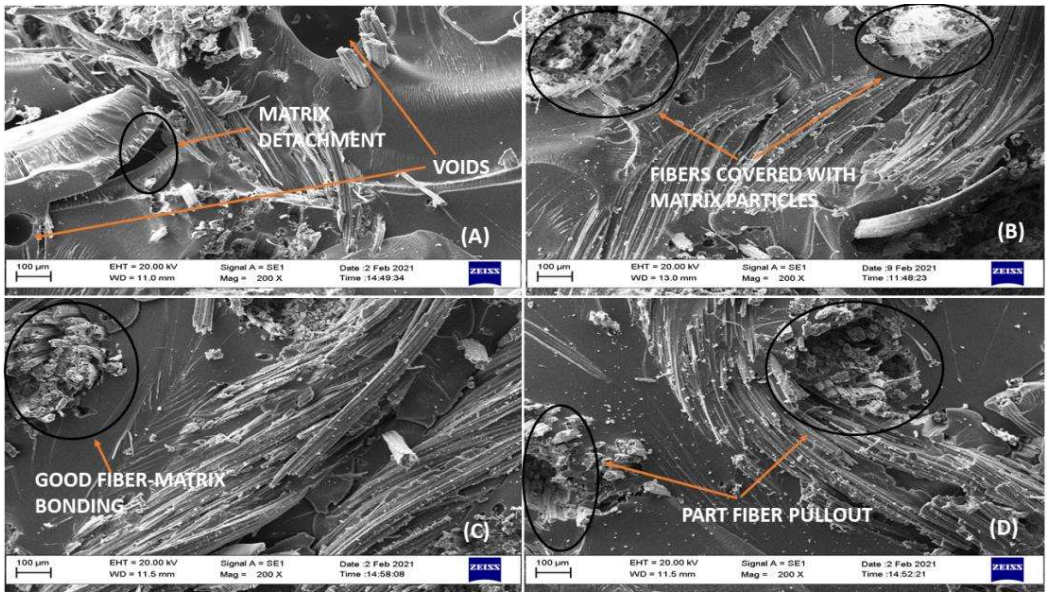

Figure 5.18 SEM images of tensile fractured surfaces of jute fiber reinforced epoxy composites (JFREC): (A) UT JFREC, (B) AT JFREC, (C) ST JFREC and (D) SHT JFREC.

5.2.4.1 Scanning electron microscopy analysis of tensile fracture surfaces

SEM images of tensile fracture surfaces of untreated UT JFREC, AT JFREC, ST JFREC and SHT JFREC are represented in Fig. 5.18. Untreated JFREC surface (Fig. 5.18(A)) shows the presence of air trappings or voids originating from the weak fiber-matrix bonding responsible for poor tensile strength. As the tension is applied, it allows the fibers to be easily pulled out from the epoxy, opening new gaps or holes in the material behind. This may have contributed to poor mechanical properties of untreated JFREC because of poor stress transfer. It is also evident from Fig. 5.18(B,C,D) that the fibers reside in the matrix and are firmly bound to the matrix even after fracture. This suggests that the chemical modification has led to better

interfacial adhesion which contributed to the enhancement in mechanical properties of treated JFREC [106,107]. Fig. 5.18(B,C,D) shows that the treated JFREC fracture surface appears relatively smooth and have a smaller void content in comparison to untreated composites.

5.2.5 Influence of chemical treatment on flexural properties of SFREC

Flexural strength and flexural modulus of untreated SFREC, SAT SFREC and SCT SFREC are shown in Fig. 5.19(A) and Fig. 5.19(B). Flexural properties (both strength and modulus), like tensile properties, follow a similar pattern. The flexural strength and flexural modulus of SAT SFREC are 8.5% and 19.1% higher than those of untreated SFREC, respectively, whereas SCT SFREC has the maximum value of flexural strength (181.63 MPa) and flexural modulus (9.36 GPa), which are 13.1% and 21.9% greater than those of untreated SFREC, respectively. The greatest flexural characteristics in SCT SFREC may be attributable to excellent stress transmission from matrix to fibers due to improved interfacial bonding between SCT fibers and matrix [46]. This can be explained by the interaction between polar sisal fibers and non-polar epoxy matrix in untreated SFREC, which results in typically weak interfacial adhesion [111]. Sisal fibers treated with sodium citrate act partially as non-polar and give improved adherence to polymeric matrix, resulting in an enhancement in flexural properties.

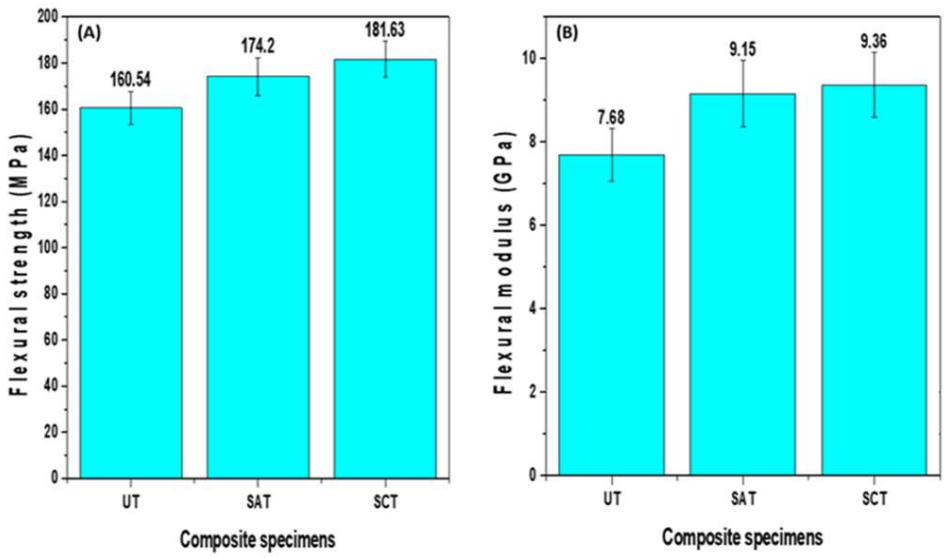

Figure 5.19 Flexural properties sisal fiber reinforced epoxy composites (SFREC): (A) Flexural strength of UT SFREC, SAT SFREC and SCT SFREC. (B) Flexural modulus of UT SFREC, SAT SFREC and SCT SFREC

5.2.5.1 Scanning electron microscopy analysis of flexural fracture surfaces

SEM micrographs of fractured samples under flexural load for untreated and treated SFREC are shown in Fig. 5.20 (at 500X) and Fig. 5.21 (at 200X). Cavities formed by fiber pullout are easily visible in the SEM images of untreated SFREC (Fig. 5.20(A)). The fracture surface of the composites treated with stearic acid (Fig. 5.20(B)) exhibits fibre breakage, however the fibers appear to remain intact with the polymer matrix. This suggested that the fibre and matrix were well-bonded. Flexural load causes some cleavage structures as well. For the sodium citrate-treated fiber composite, fiber bending occurred rather than breaking (Fig. 5.20(C)). When compared to untreated composites, the formation of grooves or fissures on the surface of treated composites is minor. The strength of the fibers rises as a result of the treatment, and they can now bear flexural loads without substantial damage.

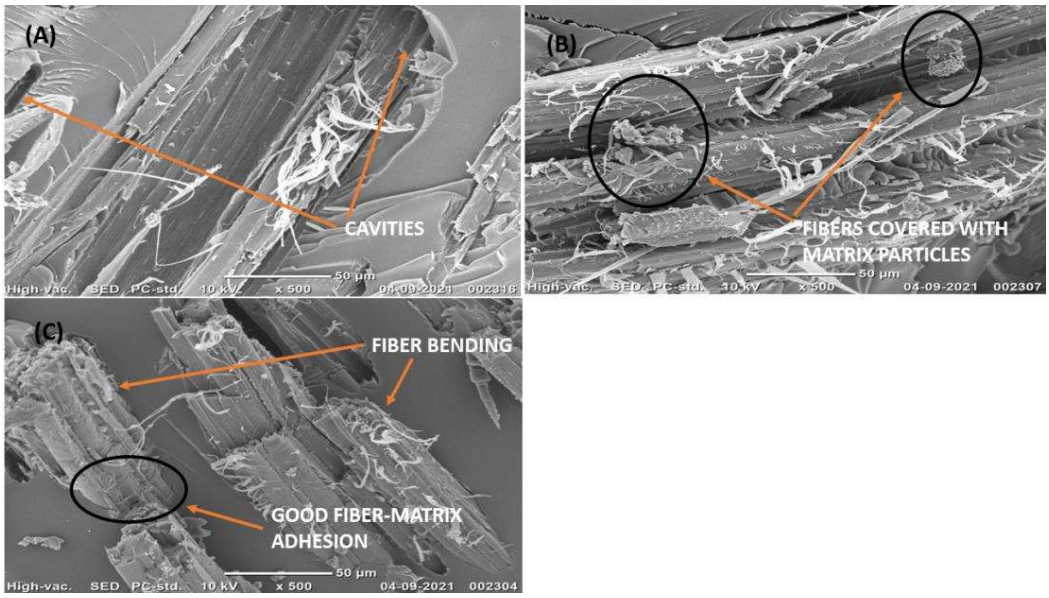

Figure 5.20 SEM images of flexural fractured surfaces of sisal fiber reinforced epoxy composites (SFREC) at 500X: (A) untreated SFREC, (B) SAT SFREC, and (C) SCT SFREC

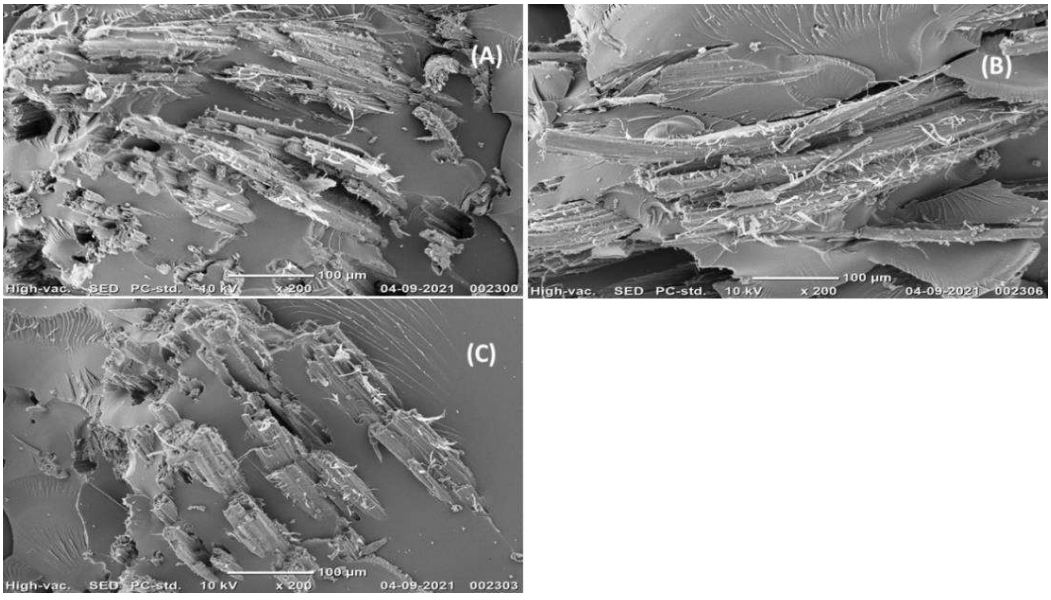

Figure 5.21 SEM images of flexural fractured surfaces of sisal fiber reinforced epoxy composites (SFREC) at 200X: (A) untreated SFREC, (B) SAT SFREC, and (C) SCT SFREC

5.2.6 Influence of gluatamic acid coating on flexural properties of SFREC

Fig. 5.22 represents influence of gluatamic acid coating on flexural properties of untreated (UT), alkali treated (AT), glutamic acid treated (GT) and combination of alkali and glutamic acid treated (AGT) SFREC. Flexural strength and modulus of the untreated SFREC are 155.23 MPa and 5.89 GPa, respectively. Chemically modified SFREC had better flexural characteristics than untreated SFREC. In comparison to UT SFREC, AT SFREC and GT SFREC improved their flexural strength by 7.8% and 3.2%, respectively. Similarly, AT SFREC and GT SFREC improved flexural modulus by 40.1% and 21.2%, respectively when compared to UT SFREC. The flexural properties of SFRECs are affected by the fiber-matrix contact as well as the strength and stiffness of both constituents [111]. Changes in fiber morphology and chemical composition during alkalization and glutamic acid treatment can be argued to alter fiber strength and interfacial characteristics between fiber and matrix in a positive way. Epoxy composites reinforced with AGT fibres have greater strength and modulus than AT and GT SFRECs. The flexural strength of AGT SFREC is found to be approximately 6.8% more than that of AT SFREC. Furthermore, the flexural modulus of the AGT SFREC is around 16% greater than that of the AT SFREC. The combination of alkali and glutamic acid treatment may remove certain hemicellulose, waxy compounds, and contaminants from the fiber surface, influencing fiber shape. Improvements in fibre mechanical characteristics may be owing to the leaching out of materials which can be dissolved in alkali solutions such as dirt as well as some part of lignin and hemicellulose. This may improved the fiber-matrix bonding which may have resulted in highest flexural properties of AGT SFREC among all the flexural tested samples.

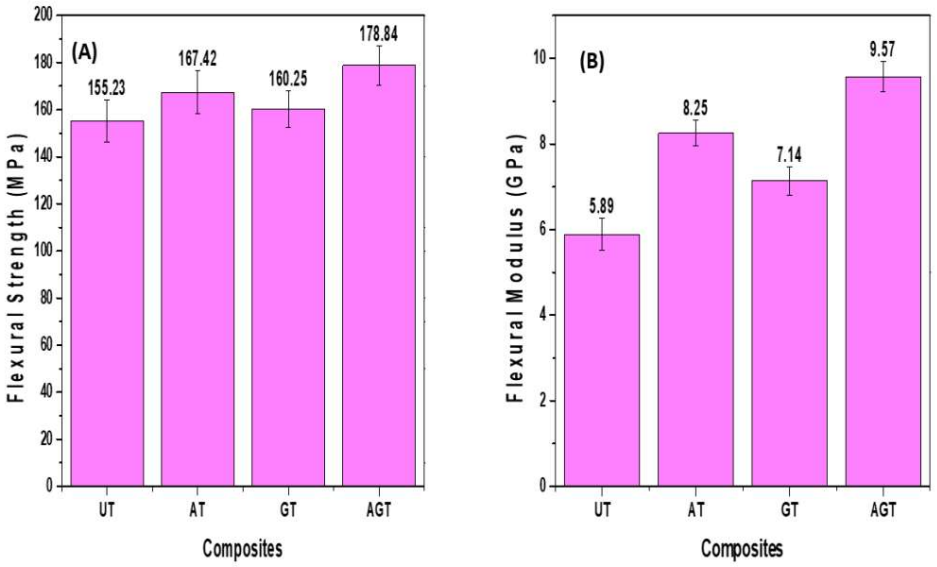

Figure 5.22 Flexural properties sisal fiber reinforced epoxy composites (SFREC): (A) Flexural strength of UT SFREC, AT SFREC, GT SFREC and AGT SFREC. (B) Flexural modulus of UT SFREC, AT SFREC, GT SFREC and AGT SFREC.

5.2.6.1 SEM observations of flexural fracture surfaces of SFREC

SEM images of fracture surfaces from the flexural tests are represented in Fig. 5.23. Compared to the untreated SFRECs, fracture surfaces of the treated SFRECs appears to be more smooth and uniform. Fiber breakage as well as cavities formed by the fiber pullout are clearly visible for the fracture surface of the untreated samples (Fig. 5.23(A)). Fracture surfaces of the untreated SFREC also have many grooves. It could have arisen from improper fiber-matrix bonding. The SEM image (Fig. 5.23(B,C,D)) also shows that there is minimal evidence of fiber pull out, indicating that chemical treatments resulted in good interfacial adhesion between the fiber and matrix, prompting enhanced propagation of stress from fiber to matrix and vice-versa.

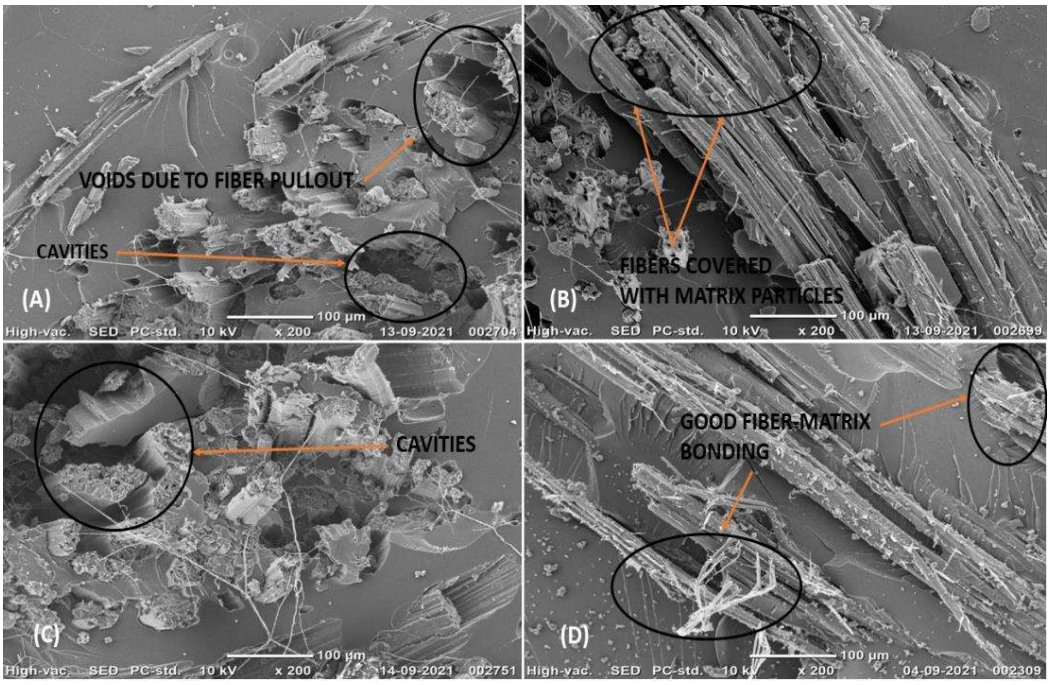

Figure 5.23 SEM images of flexural fractured surfaces of sisal fiber reinforced epoxy composites (SFREC): (A) UT SFREC, (B) AT SFREC, (C) GT SFREC and (D) AGT SFREC.

5.2.7 Effect of fiber coatings on impact properties of HFREC

Charpy impact strength of uncoated, PHB coated, and PLA coated hemp fiber composites were displayed in Fig. 5.24. From the Fig. 5.24, it is observed that similar to the tensile properties, the impact strength of PHB coated, and PLA coated hemp fiber composites also showed an improvement of 40.2% and 47.8% in comparison to the impact strength of uncoated fiber composites. The fibrillation of elementary fibers due to the sodium hydrogen carbonate treatment results in a greater interfacial area and the deformation of the ductile polymer coating around the fibers during the fracture of the specimens may have absorbed some energy, allowing the impact energy of these specimens to be larger than the uncoated hemp fiber composites [112-114].

5.2.8 Effect of glutamic acid coatings on impact properties of SFREC

The impact strength values of UT SFREC, AT SFREC, GT SFREC and AGT SFREC are shown in Fig. 5.25. From Fig. 5.25, it is observed that the impact strength of SFREC increases appreciable after chemical treatment. There is an increament of 31.7%, 41.3% and 22.6% in impact strength of AT SFREC, GT SFREC and AGT SFREC in comparison with UT SFREC. Improved fiber–matrix bonding due to the surface modification of the sisal fibers makes it difficult for the fiber to be pulled out from the matrix material. So, a larger amount of energy is consumed by the composite before fracture.[113] This may be the possible explanation for the untreated composites to have lesser impact strength.

5.2.9 Influence of chemical treatment on impact properties of JFREC

Fig. 5.26 shows the charpy impact strength of both treated and untreated JFREC. As in case with tensile strength of JFREC, the impact strength also improves by about 22.6%, 41.3%, and 31.7% for sodium hydroxide, sodium carbonate, and sodium hydrogen carbonate treated jute fiber reinforced composites relative to untreated composites. The chemical treatment causes elementary fibers to fibrillate, resulting in a larger interfacial area that may have absorbed some energy during specimen fracture, allowing the impact energy of these specimens to be higher than untreated jute fiber composites [112,114]. This may be the possible explanation for lesser impact strength of untreated JFREC in comparison to treated JFREC. However, this proves that the chemical modifications have promoted the enhancement of matrix-fibre adhesion.

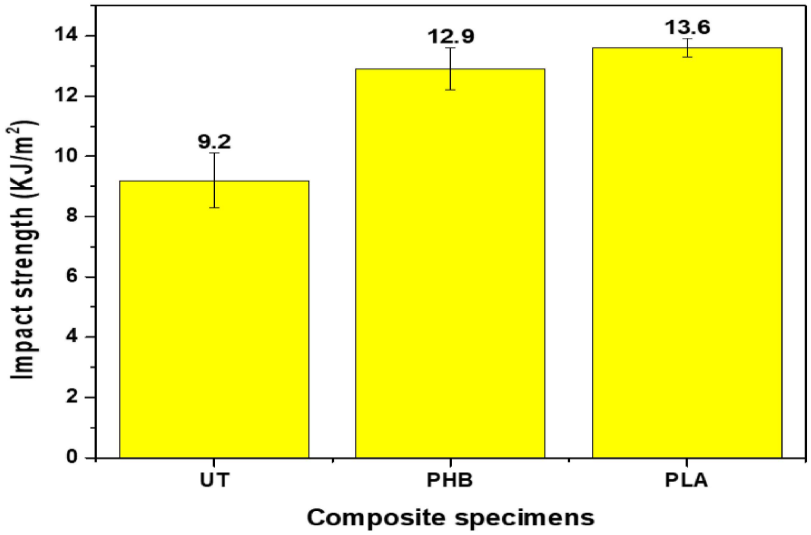

Figure 5.24 Impact strength of uncoated HFREC, PHB coated HFREC, and PLA coated HFREC.

5.2.10 Influence of chemical treatment on Inter-laminar shear strength (ILSS) properties of SFREC

Short beam shear test was used to determine the inter-laminar shear strength (ILSS) of the SFREC. The ILSS of the untreated and treated SFREC were shown in Fig. 5.27. Both the chemical treatment improves the ILSS of the treated SFREC in comparison to the untreated SFREC. These findings are in line with other mechanical properties. The composites prepared with SAT fibers showed an improvement of 29.4% in ILSS over untreated SFREC. The elimination of natural and manufactured contaminants from the fiber surface by stearic acid treatment increases fiber-matrix adhesion [99]. Untreated SFREC exhibited the lowest ILSS among all the composites. It is commonly recognized that the lowest ILSS results from insufficient fiber-matrix interaction due to the presence of surface impurities in untreated fibers [115]. The composite reinforced with SCT fibres showed the greatest improvement in ILSS, which was approximately 51.2% greater than the untreated SFREC. Fiore et al. [67]

underlined that the sodium citrate treatment improves not only fibre strength but also fiber-matrix adhesion by roughening the fibre surface and decreasing the hydrophilic behaviour of the fibres, resulting in enhanced mechanical interlocking.

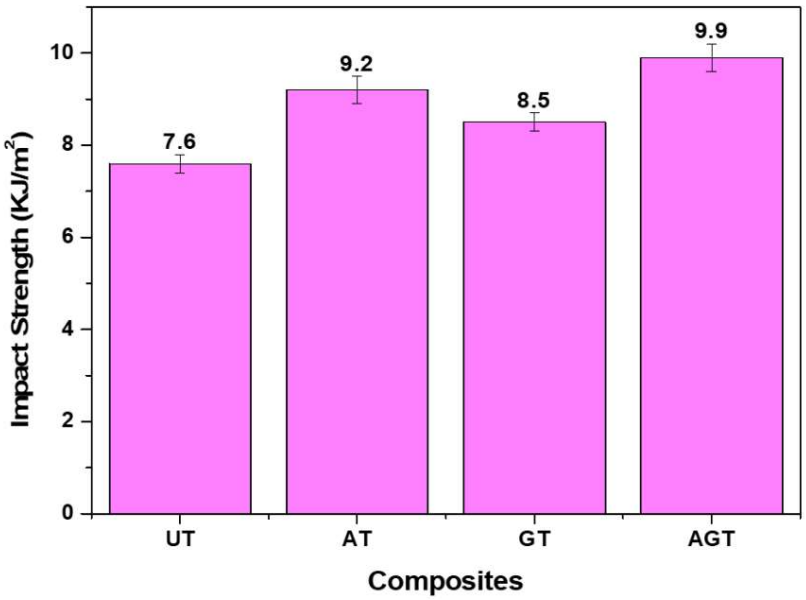

Figure 5.25 Impact strength of UT SFREC, AT SFREC, GT SFREC and AGT SFREC.

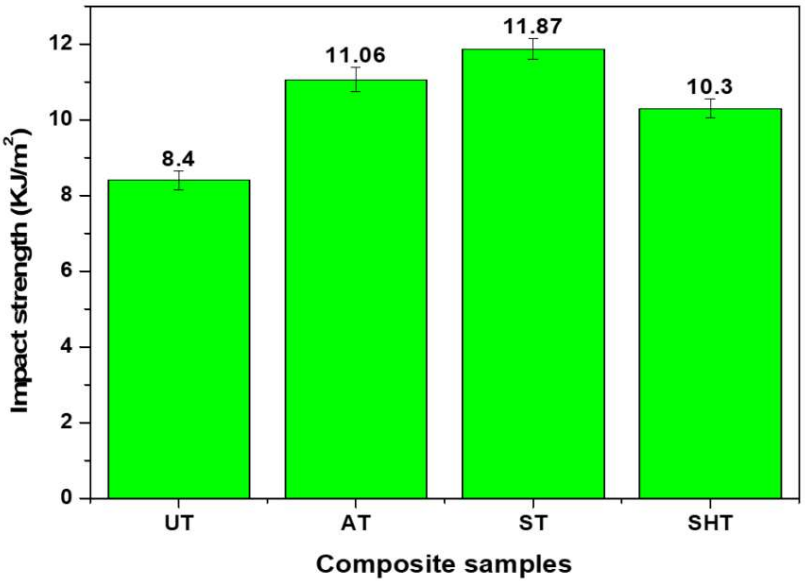

Figure 5.26 Impact strength of UT JFREC, AT JFREC, ST JFREC and SHT JFREC.

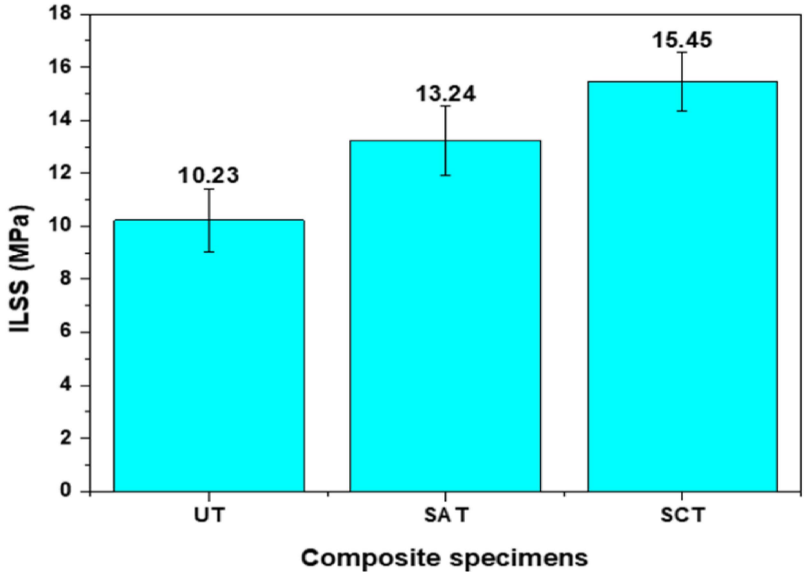

Figure 5.27 ILSS of UT SFREC, SAT SFREC and SCT SFREC.

5.2.11 Influence of chemical treatment on micro-hardness properties of HFREC

Vickers microhardness values of UT, ST, and PT HFREC are shown in Table 5.1. From Table 5.1, it is quite evident that the micro-hardness values of treated HFREC were higher than of UT HFREC. There is an improvement of 7.9% and 15.1% in micro-hardness values of ST and PT HFREC when compared to UT HFREC. Enhanced wettability between chemically treated hemp fiber and epoxy resin is the possible reason for this improvement in micro-hardness properties of treated HFREC [116].

Table 5.1 Vickers microhardness values of untreated and treated HFREC

Composite specimens	Microhardness (HV)
UT HFREC	15.76 ± 0.89
ST HFREC	17.01 ± 0.96
PT SFREC	18.13 ± 0.90

5.2.12 Effect of fiber coatings on micro-hardness properties of HFREC

Micro-hardness values from the Vickers micro-hardness tests of uncoated, PHB coated, and PLA coated hemp fiber composites were represented in Table 5.2. It can be observed from the Table 5.2 that the coated HFREC had higher micro-hardness values than the uncoated HFREC. There is an enhancement of 21.3% and 28.2% in micro-hardness values of PHB coated and PLA coated hemp fiber composites, respectively, in comparison to uncoated fiber composites. The possible reason for such increase in microhardness values of coated HFREC is the improved bonding between the polymer (PHB and PLA) coated fiber and the epoxy resin [116].

Table 5.2 Vickers microhardness (HV) values of uncoated and coated HFREC

Composite specimens	Microhardness (HV)
UT HFREC	16.36 ± 0.91
PHB coated HFREC	19.85 ± 0.86
PLA coated HFREC	20.98 ± 0.52

5.2.13 Effect of glutamic acid coatings on the micro-hardness properties of SFREC

Vickers microhardness tests of SFREC were performed at a test load of 300 gm with the help of a micro-indentation tester. AT SFREC had a maximum hardness value of 21.23 HV followed by AGT SFREC, GT SFREC, and UT SFREC with hardness value of 19.05 HV, 18.06 HV, and 17.76 HV, respectively. This slight increase in hardness value of treated SFREC can be due to the improved wettability between the chemically modified fibers and the matrix [116].

5.3 Tribological properties of natural fiber reinforced epoxy composites

Researchers have been drawn to examine the viability of using natural fibers as reinforcement and the extent to which they meet the necessary requirements in tribological applications because of their accessibility, biodegradability and ease of manufacturing. The employment of NFRECs in tribological application has also introduced the concept of 'green tribology', whose main aim is to reduce the impact on the environment without compromising our needs. Friction and wear are the two major factors that primarily determines the tribological properties of any material. This research will focus on the the influence of various chemical treatment on the fiber surface and fiber coating on the tribological behaviour of NFRECs.

5.3.1 Effect of operating parameters and chemical treatment on tribological properties of HFREC

5.3.1.1 Specific wear rate (SWR)

Fig. 5.28(A) shows the SWR of UT, ST, and PT HFREC at different applied loads (20, 25, 30, and 35 N) under a constant sliding speed of 1.3 m/s. It can be observed from Fig. 5.28(A) that the SWR of all the composite samples (both treated and UT) increases with the increase in applied load. Several researchers have also reported similar observations in their research articles [55,117,118]. This can be due to the thermal softening of the epoxy matrix as a result of excessive heat generation at the interface of the composite and counter surface, which may have contributed to the excessive material loss [119]. Also at a higher load, there is a greater chance of detachment of the lubricant film, which is also responsible for excessive material loss [120]. At 20 N normal load, the PT HFREC exhibited the lowest SWR of 0.0072 mm^3/Nm and at 35 N normal load, and the UT HFREC exhibited the highest SWR of 0.0186 mm^3/Nm.

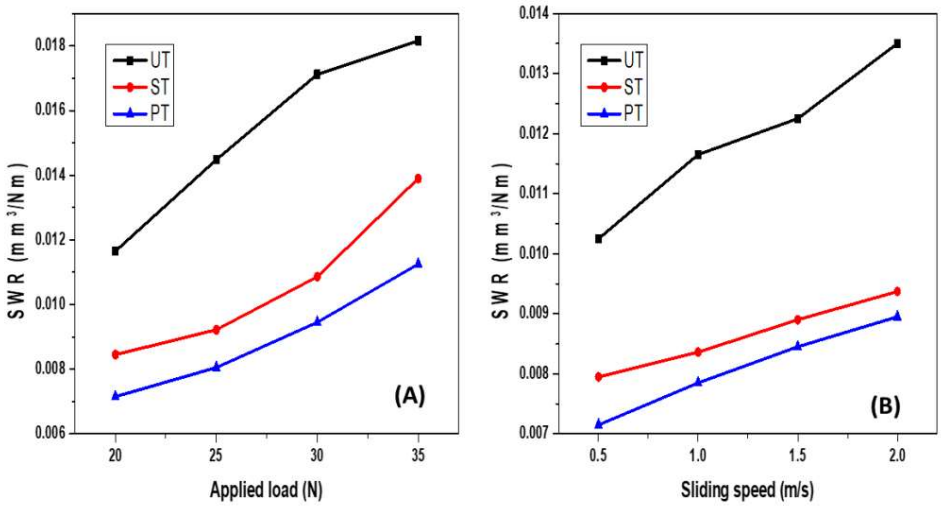

Figure 5.28 Tribological properties of HFREC (A) SWR vs Applied load and (B) SWR vs Sliding speed

Fig. 5.28(B) shows the SWR of UT, ST, and PT HFREC at different sliding speeds (0.5, 1, 1.5, and 2 m/s) under a uniform applied load of 25 N. As in the case with applied load, the SWR of all the HFREC samples also increases with the increase in sliding speed. Greater frictional heat production at higher sliding speed is responsible for lowering the polymer's wear resistance. This may be the reason for increased SWR at higher speeds [121]. At 0.5 m/s sliding speed, the PT HFREC exhibited the lowest SWR of 0.0046 mm^3/Nm and at 2 m/s sliding speed, the UT HFREC exhibited the highest SWR of 0.0135 mm^3/Nm. It was also observed from Fig. 5.28(A,B) that both the ST and PT HFREC composites showed lower SWR in comparison with UT composites. It may be possible that both the sodium carbonate and peroxide treatment have reduced the hemicellulose and lignin content of the hemp fiber resulting in the splitting of the fiber. This change in fiber structure caused an improvement of cellulose content and removal of surface impurities like wax, and the splitting of the fiber resulted in an improvement of surface roughness of fibers. This may have

enhanced the interlocking or interfacial adhesion between the treated hemp fiber and the epoxy matrix by increasing the hemp fiber's interacting area with the matrix [122,123]. Fig. 5.28(A,B) also revealed that the maximum wear resistance was shown by PT HFREC, followed by ST HFREC and UT HFREC.

5.3.1.2 Coefficient of friction

A typical curve of the coefficient of friction (COF) as function of the time for the composites are presented in Fig. 5.29. Shown are the COF vs time curves of the UT HFREC, ST HFREC and PT HFREC (Fig 5.29). According to the results, the COF values range between 0.5 and 0.3. These values are of the same order of magnitude for those presented in the literature for dry sliding wear in other composites of polymer resin reinforced with some other natural fibers [131-132] or glass fibers [133-134] using a steel counter-body. This may indicate that the resin is mainly responsible for the coefficient of friction of the composite against steel, while fiber has a secondary role. Results presented in Fig 5.29 show that within the range of the tribological test, the behavior of the COF is stable for all the samples tested, with no severe changes in the curves. This may indicate that no severe stick and slip process is taking part in the system. Nevertheless, oscillating behavior present in the HFREC has been found in the literature [132-133] and could be considered typical. This oscillatory phenomenon may be due to adhesion in the asperities of the interacting surfaces as has been reported by Viáfara and Sinatora [135].

Fig. 5.30(A) shows the COF values of UT, ST, and PT HFREC under a uniform sliding speed of 1.3 m/s at different applied loads (20, 25, 30, and 35 N). It can be seen from Fig. 5.30(A) that the COF of all the composite samples (both UT and treated) increases with the increase in applied load. Mylsamy et al. [124] also reported

a similar observation. There is a possibility of an increase in frictional force as a result of the enhancement in interface temperature due to the increase in contact pressure between the specimen and the steel ball at higher loads. This may be the reason for the increase in COF at higher loads [119,125]. At 20 N normal load, the PT HFREC has the lowest friction coefficient value of 0.332, and at 35 N normal load, the UT HFREC has the highest friction coefficient value of 0.541.

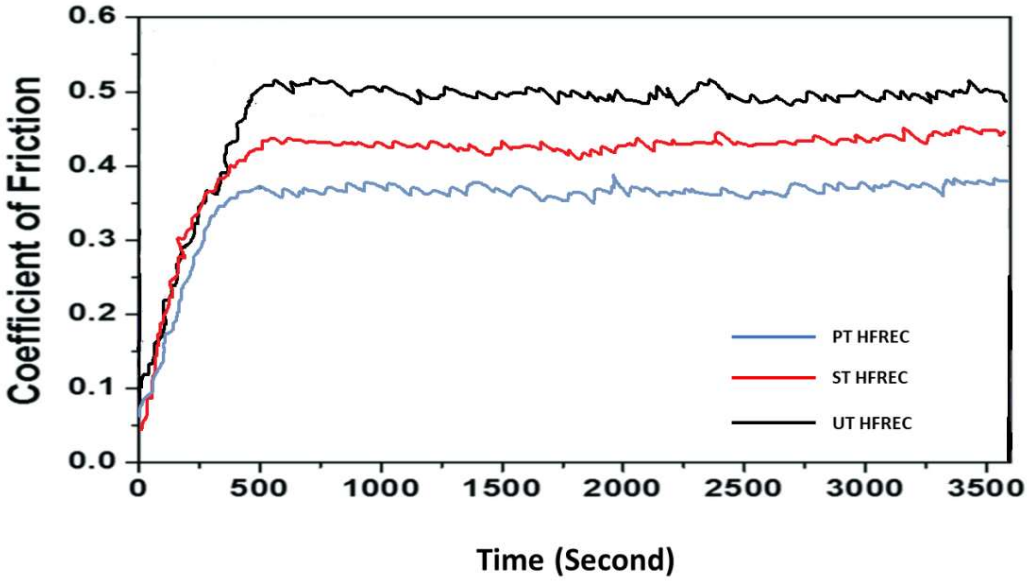

Figure 5.29 COF Vs Time graph for chemically modified HFREC

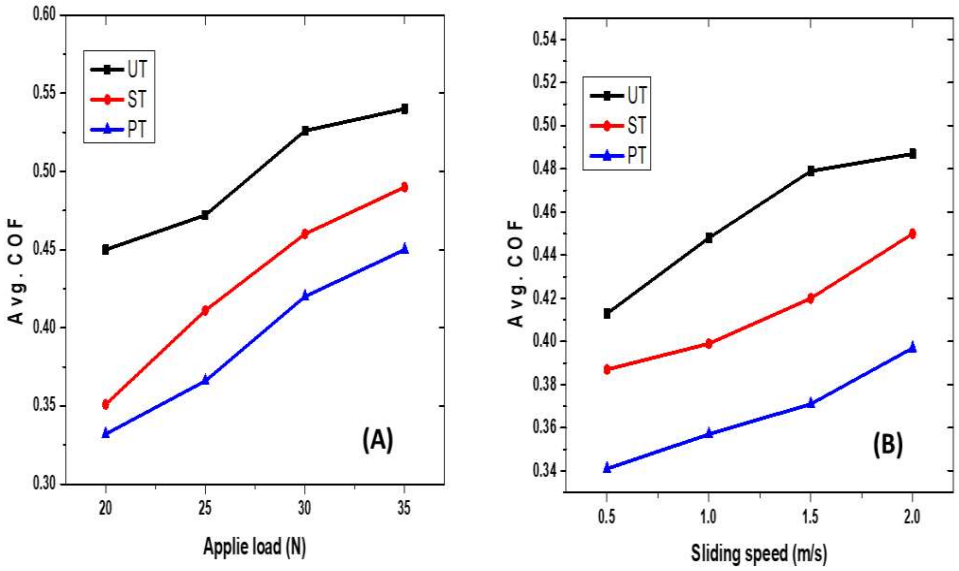

Figure 5.30 Tribological properties of HFREC (A) Avg. COF vs Applied load and (B) Avg. COF vs Sliding speed

Fig. 5.30(B) shows the COF values of UT, ST, and PT HFREC under a constant applied load of 25 N at different sliding speeds (0.5, 1, 1.5, and 2 m/s). As in the case with applied load, the COF values of all the tested HFREC specimens also increase with the increase in sliding speed. There will be an enhancement of frictional force due to the increase in interface temperature at higher speeds [119]. This may be the reason for the increase in COF at higher speeds. The lowest COF value of 0.341 was obtained for PT HFREC at 0.5 m/s and the highest COF value of 0.487 was obtained for UT HFREC at 2 m/s. It was also observed from Fig. 5.30(A,B) that the friction coefficient values of both ST and PT HFREC were lower in comparison with the COF values of UT HFREC. Improvement in interfacial adhesion between the treated fiber and the epoxy due to the sodium carbonate and peroxide treatment of the fiber results in the development of lubricant film during the wear process, which reduces the

material loss and improves the frictional properties [51,57]. Fig. 5.30(A,B) also revealed that the most desired COF values (0.3–0.5) under industrial norms for brake pads were obtained for PT HFREC, followed by ST HFREC and UT HFREC.

5.3.1.3 SEM analysis of worn surface

SEM micrographs of the worn surfaces (at 25 N normal load and 1.5 m/s sliding speed) of UT HFREC, ST HFREC, and PT HFREC are shown in Fig. 5.31. The worn surface of UT HFREC was marked by complete separation of hemp fiber from the epoxy matrix resulting in a large interface gap between fiber and the matrix (Fig. 5.31(A)). Lots of wear debris and excessive fiber cutting can also be seen on the worn surface of UT HFREC, which also signifies poor wear resistance of UT HFREC [51,56]. Also during the wear process, a considerable amount of wear debris was also observed on the counterpart surface. The wear process was adhesive in nature; however, it may have converted into abrasive after the fiber pullout from the epoxy matrix in case of UT HFREC[57]. The worn surfaces of both ST HFREC and PT HFREC were found to be comparatively smoother than the wear surface of UT HFREC. The worn surface of treated HFREC was also characterized by the lighter plow and adhesion spots and proper attachment of hemp fibers with the epoxy matrix, which resonated to the better fiber–matrix adhesion due to the chemical modification (Fig. 5.31(B,C)). The worn surface of PT HFREC was also marked by a thin transfer film, which reduces the material removal rate (Fig. 5.31(C)). This may be the reason for the best wear resistance of PT HFREC among all the tested composites. Also, it can be observed from the worn surface of treated HFREC (Fig. 5.31(B,C)) that plowing is the dominant wear feature in surface-treated composites.

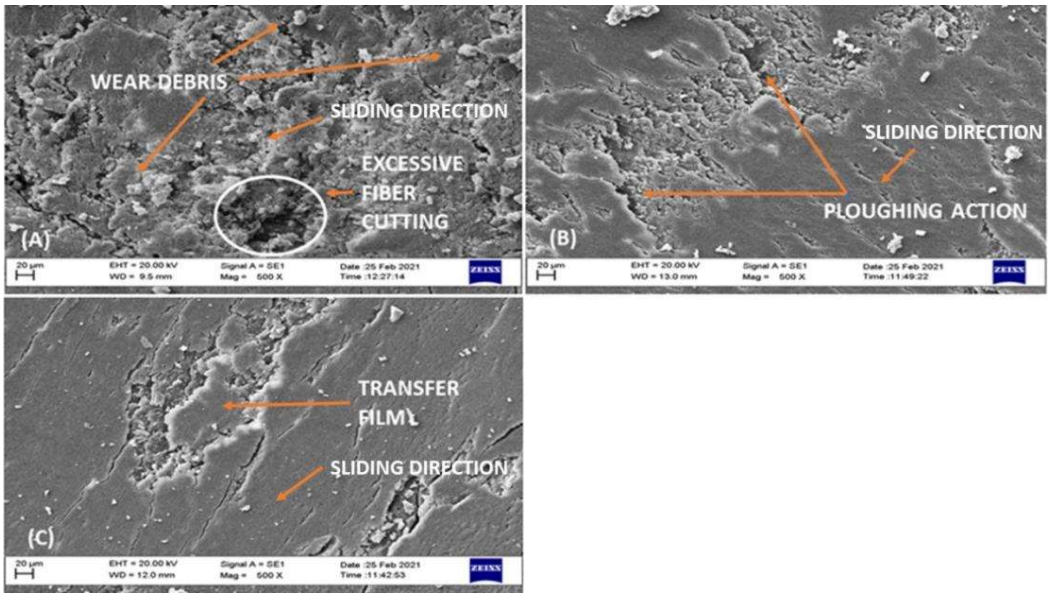

Figure 5.31 SEM images of worn surfaces of hemp fiber reinforced epoxy composites (HFREC) at 25 N load and 1.5 m/s sliding speed: (A) UT HFREC, (B) ST HFREC, and (C) PT HFREC

5.3.2 Effect of operating factors and fiber coatings on tribological properties of HFREC

5.3.2.1 Specific wear rate (SWR)

The impact of normal loads (15 N, 20 N, 25 N, and 30 N) on the SWR of uncoated HFREC, PHB coated HFREC, and PLA coated HFREC at constant sliding speed of 2.7 m/s are displayed in Fig. 5.32(A). It can be noticed from the Fig. 5.32(A) that the increase in applied load increases the SWR of both uncoated HFREC and coated HFREC samples. Several researchers had also obtained similar results in their research work [55,117,118]. At higher loads, a close adhesion force forms between the composite specimens and the surface of the steel ball; these atomic forces are much more intense than both the materials innate properties and thus breaking the bonds, which results in higher SWR in weaker material [120]. Increased material loss from the composite surface can also be due to the removal of lubricant layer at higher

load [126]. The PLA coated fiber composites exhibited minimum SWR of 0.0061 mm^3/Nm at 15 N normal load and the uncoated HFREC exhibited the maximum SWR of 0.0365 mm^3/Nm at 30 N normal load among all the composites tested at different applied loads.

The effect of siding speeds (2 m/s, 2.5 m/s, 3 m/s, and 3.5 m/s) on the SWR of uncoated HFREC, PHB coated HFREC, and PLA coated HFREC at constant applied load of 20 N are displayed in Fig. 5.32(B). As with applied load, the SWR of both uncoated and coated fiber composite samples also increases as the sliding speed increases. Increased material loss from the composite surface at higher speed can be due to the thermal softening of the epoxy layer as a result of higher frictional heat generation at the interface [121]. The PLA coated fiber composites exhibited minimum SWR of 0.0055 mm^3/Nm at 2 m/s sliding speed and the uncoated HFREC exhibited the maximum volume loss of 0.0251 mm^3/Nm at 3.5 m/s sliding speed among all the composites tested at different sliding speeds. It can also be observed from Fig. 5.32(A,B) that both the coated HFREC showed higher wear resistance in comparison to uncoated HFREC. It can be possible that the prior treatment of fiber with sodium hydrogen carbonate may have improved the fibers'surface roughness and the polymer coating (PHB and PLA) of the fiber may have reduced its hydrophilic nature contributing to its improved mechanical interlocking with epoxy matrix [44,45,51,124]. This may be the possible explanation for the increased wear resistance of the coated HFREC. From Fig. 5.32(A,B), it was also observed that the PLA coated HFREC showed the lowest SWR, followed by PHB coated HFREC and uncoated HFREC.

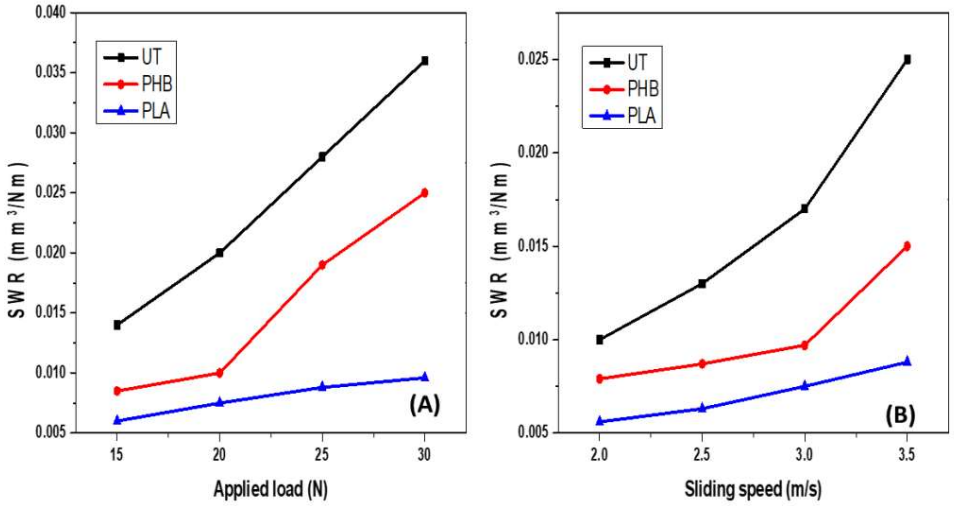

Figure 5.32 Tribological properties of polymer coated HFREC (A) SWR vs Applied load and (B) SWR vs Sliding speed

5.3.2.2 Coefficient of friction

Fig. 5.33 presents a typical curve for the composites' coefficient of friction (COF) as a function of time. The COF vs. time curves for the UT HFREC, PHB HFREC, and PLA HFRECs are displayed in Fig. 5.33. The results show that the COF values fall between 0.45 and 0.25. These numbers are in the same region as those for dry sliding wear in other polymer resin composites reinforced with various other natural fibres [131-132] or glass fibres [133-134] that use a steel counter-body. This may suggest that fibre plays a supporting function to resin in determining the composite's coefficient of friction with steel. Results shown in Fig 5.33 demonstrate that the COF behaviour is stable for all tested substances within the tribological test range, with no significant variations in the curves. This can mean that the system is not experiencing a severe stick and slip process. However, the fluctuating behaviour shown in the HFREC has been documented in the literature [132-133] and may be regarded as

usual. According to Viáfara and Sinatora [135], this oscillating phenomena may be caused by adhesion in the asperities of the contacting surfaces.

The effect of normal loads (15 N, 20 N, 25 N, and 30 N) on the COF values of uncoated HFREC, PHB coated HFREC, and PLA coated HFREC at a uniform sliding speed of 2.7 m/s are represented in Fig. 5.34(A). It can be observed from the Fig. 5.34(A) that the increase in applied load increases the friction coefficient values of both uncoated and coated fiber composites. Similar result was also observed by Mylsamy et al. [124] in their research work. At higher loads, the COF values increases due to the increase in friction force as a result of the rise in interface temperature due to the increased contact pressure between the composite specimen and the steel ball [119,125,127]. The lowest value of COF was obtained for PLA coated HFREC at 15 N applied load was 0.32 and the highest value of COF was obtained for uncoated HFREC at 30 N applied load was 0.49 among all the composites tested at different applied loads.

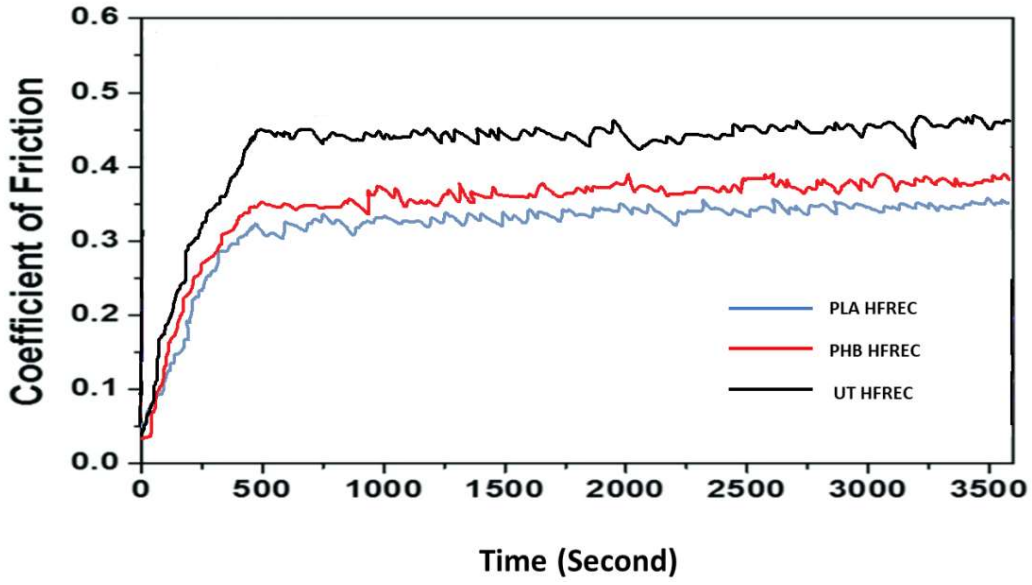

Figure 5.33 COF Vs Time graph for polymer coated HFREC

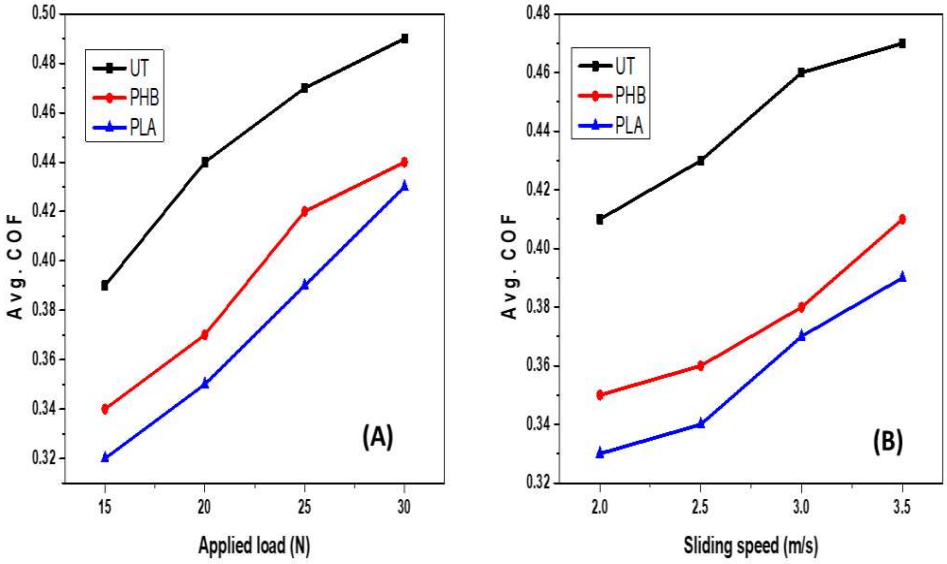

Figure 5.34 Tribological properties of polymer coated HFREC (A) Avg. COF vs Applied load and (B) Avg. COF vs Sliding speed

The effect of sliding speeds (2 m/s, 2.5 m/s, 3 m/s, and 3.5 m/s) on the COF values of uncoated HFREC, PHB coated HFREC, and PLA coated HFREC at a constant applied load of 20 N are displayed in Fig. 5.34(B). As with applied load, the friction coefficient values also increases with the increase in sliding speed for both the uncoated and coated fiber composites. At higher speeds, the amount of heat generated at the interface between the HFREC specimen and the steel ball increases causing the frictional force to rise which results in the enhancement of COF values [119]. The lowest friction coefficient value of 0.33 was acquired for PLA coated fiber composites at 2 m/s sliding speed and the highest friction coefficient value of 0.47 was acquired for uncoated fiber composites at 3.5 m/s sliding speed. It was also noticed from the Fig. 5.34(A,B) that the friction coefficient values of PHB coated and PLA coated fiber composites were lower than the COF values of uncoated fiber

composites. Enhancement of mechanical interlocking between the hemp fiber and epoxy matrix owing to the sodium hydrogen carbonate treatment and polymer coating of the fiber resulted in the formation of friction film which may have reduced the material loss and COF values [51,56]. From the Fig. 5.34(A,B), it was also observed that the most desired COF values (0.3–0.5) under industrial norms for break pads was obtained for PLA coated hemp fiber composites, followed by PHB coated fiber composites and uncoated fiber composites.

5.3.2.3 Scanning electron microscopy analysis of worn surface

SEM images of the wear surfaces of the uncoated, PHB coated, and PLA coated HFREC were displayed in Fig. 5.35. Wide interface gap created between the fiber and the matrix due to the detachment of the fiber from the matrix was observed on the wear surface of uncoated fiber composite in Fig. 5.35(A). The wear surface of the uncoated HFREC was also marked by extreme fiber cutting and wear debris from both the fiber and the matrix [51,126]. This validates the poor wear resistance of uncoated HFREC among all the wear tested composites. The nature of the wear process was adhesive in the beginning but due to the fiber pullout it may have converted into abrasive wear [56].

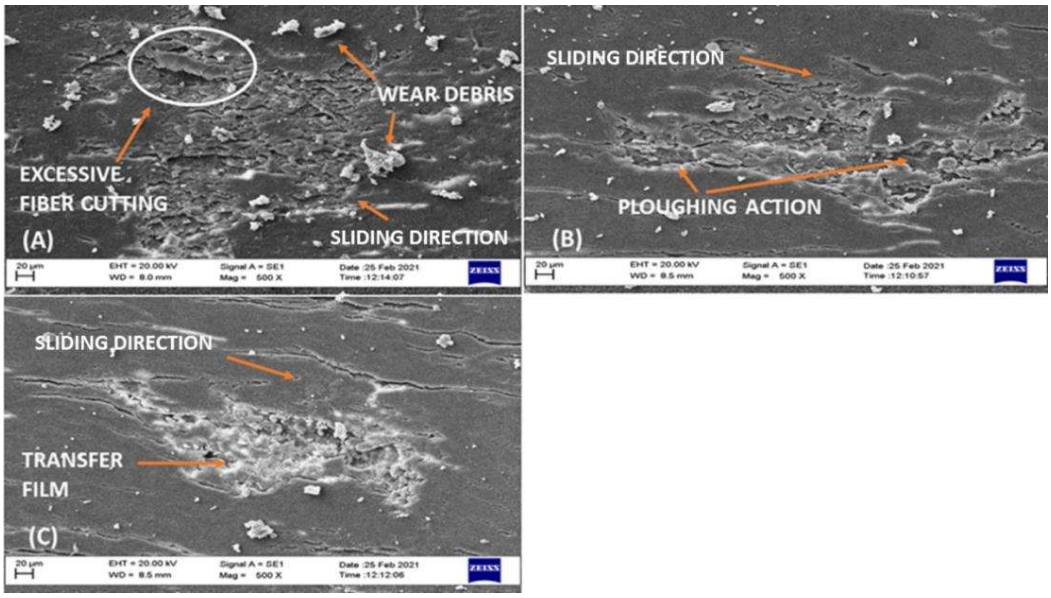

Figure 5.35 SEM images of worn surfaces of HFREC at 20 N load and 2.7 m/s sliding speed: (A) Untreated HFREC, (B) PHB coated HFREC, and (C) PLA coated HFREC.

Comparatively, smooth wear surface was observed for PHB coated HFREC and PLA coated HFREC in the Fig. 5.35(B,C). From the Fig. 5.35(B,C), it was also observed that the hemp fibers were properly attached to the polymer matrix due to the improved fiber-matrix bonding as a result of the polymer coatings of the fibers. Plowing marks and the adhesion spots were also less visible on the wear surface of the coated fiber composites. The wear surface of the coated fiber composites were also characterized by the presence of thin transfer film, which may have improved their wear resistance. Plowing may be considered as the primary wear feature in polymer coated HFREC as observed in Fig. 5.35(B,C).

5.3.3 Effect of operating parameters and chemical treatment on tribological properties of SFREC

5.3.3.1 Friction and wear

Fig. 5.36 shows curves of the coefficient of friction (COF) as a function of time for the UT SFREC, SAT SFREC and SCT SFREC. The COF levels range between 0.45 to 0.25, according to the findings. These values are comparable to those reported for dry sliding wear in other polymer resin composites reinforced with other natural fibres [131-132] that utilise a steel counter-body. This might imply that fibre aids resin in defining the composite's coefficient of friction with steel. The results in Fig. 5.36 reveal that the COF behaviour is stable for all tested compounds throughout the tribological test range, with no notable differences in the curves. This might indicate that the system is not undergoing a significant stick and slide process. However, the SFREC's oscillating conduct has been recorded in the literature [132-133] and may be considered normal. This oscillating phenomenon, according to Viáfara and Sinatora [135], might be induced by adhesion in the asperities of the contacting surfaces.

Fig. 5.37(A) show the coefficient of friction (COF) and wear rates of composites filled with untreated and treated sisal fibers under normal loads of 5N, 10N, 15N, and 20N, respectively, at a constant sliding speed of 0.52 m/s. When compared to untreated composites, the treated composites had a lower coefficient of friction. The coefficient of friction of the composites increased little during the preliminary friction stage. The transfer film between the metal counterpart and the composites was not produced at first. This could be the cause of the aforementioned phenomenon [128]. The COFs of untreated (UT) SFREC and stearic acid treated (SAT) SFREC were essentially identical, and they dramatically rose as the load increased, from about 0.34 for 5N to about 0.47 for 20N. For 10 N to 20 N load, COF varied between 0.38 and

0.42. Mylsamy et al. [124] found a similar finding in their investigation as well. The increase in friction force as a consequence of rising in interface temperature due to the higher contact pressure between the composite specimen and the steel ball causes the COF values to climb at higher loads [119,127]. However, COF of sodium citrate treated (SCT) SFREC was found to be remarkably lower than both UT SFREC and SAT SFREC under similar testing conditions. The maximum and minimum COF obtained for SCT SFREC was 0.36 and 0.23 at 20N and 5N load respectively. Because of the sodium citrate alteration of the fibre, increased mechanical interlocking between the hemp fibre and epoxy matrix resulted in the production of a friction film, which may have minimized material loss and COF values [51,56].

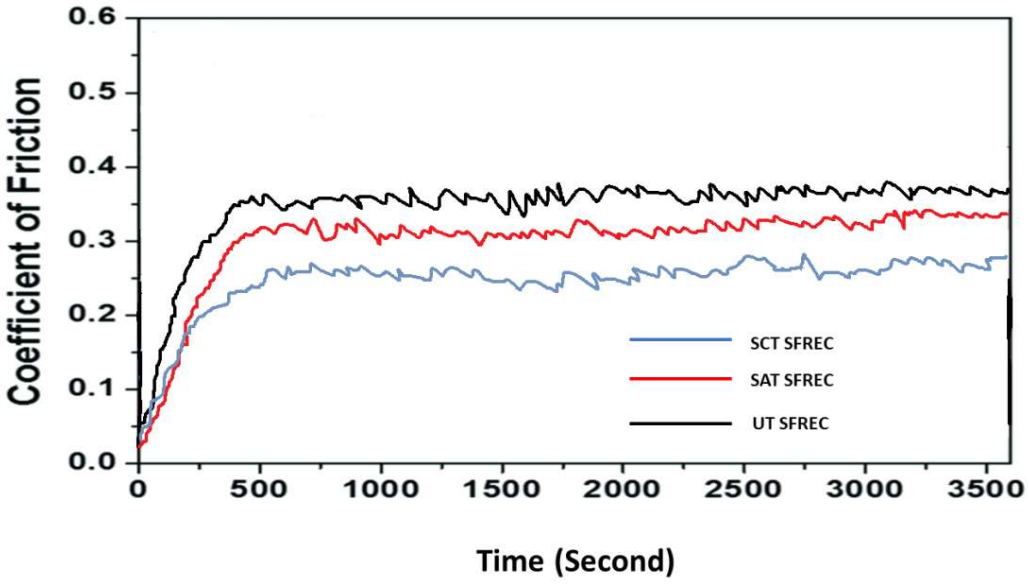

Figure 5.36 COF Vs Time graph for chemically treated SFREC

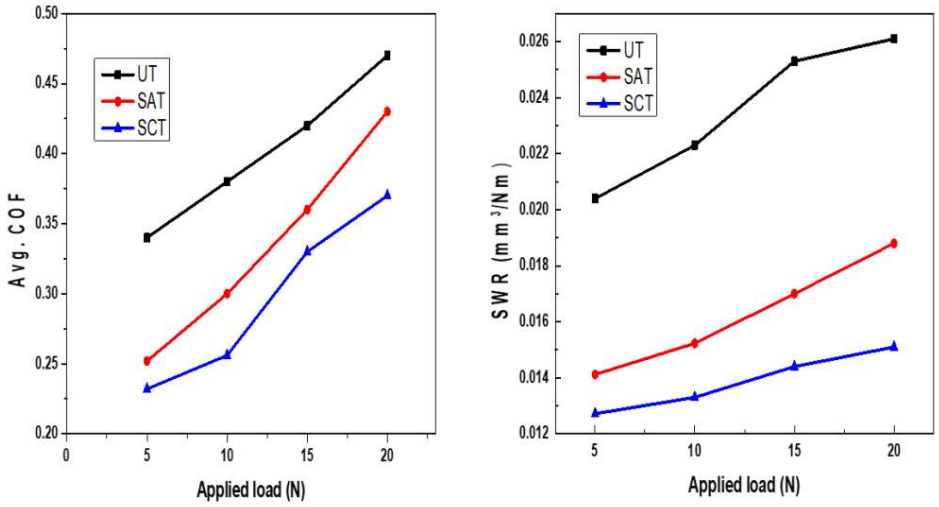

Figure 5.37 Tribological properties of SFREC (A) Avg. COF vs Applied load and (B) SWR vs Applied load

Fig. 5.37(B) shows that the SWR of both untreated and treated fibre composites increases as the load increases. At larger loads, a strong adhesion force arises between the composite sample and the steel ball's surface; these atomic forces are significantly stronger than both materials' inherent characteristics, shattering the bonds and resulting in greater SWR in the composite material. The ablation of the lubricant layer at greater loads might also cause increased material loss from the composite surface [120,126]. As the case with COF, both SAT SRFEC and SCT SFREC showed significantly lower SWR than the UT SFREC under similar testing conditions. It's probable that the fibres' surface roughness was improved by previous treatment with stearic acid and sodium acetate, which reduced their hydrophilic character, resulting in improved adhesion strength with epoxy matrix [129]. This could be one explanation for the treated SFREC's enhanced wear resistance [121,128].

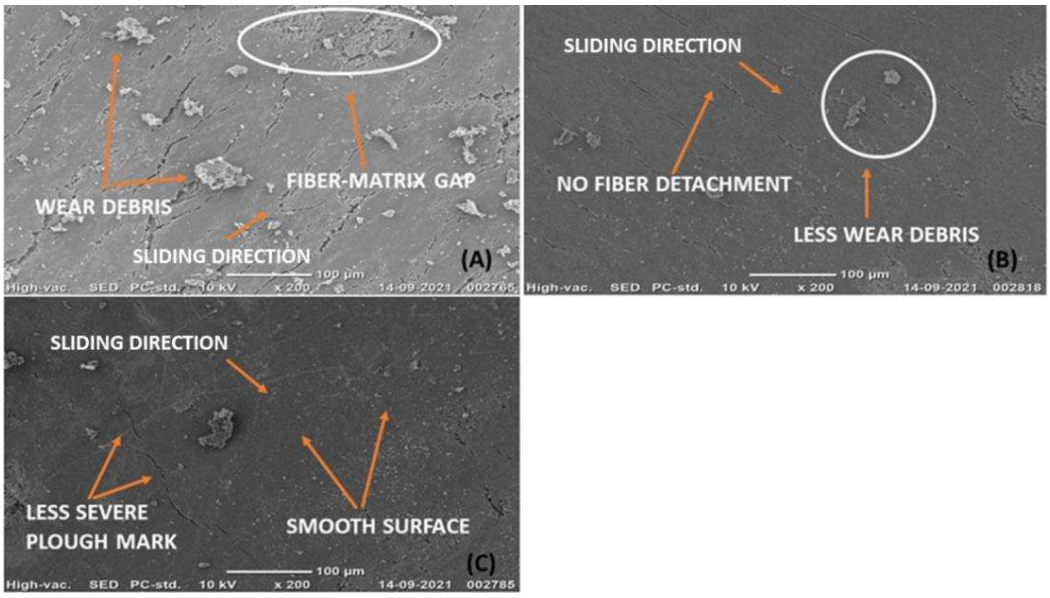

Figure 5.38 SEM images of wear surfaces of sisal fiber reinforced epoxy composites (SREC) at 15 N applied load and 0.52 m/s sliding speed: (A) untreated SFREC, (B) SAT SFREC, and (C) SCT SFREC.

5.3.3.2 SEM analysis of wear surface

SEM study of the worn surfaces of the SREC sliding against the steel ball at 0.52 m/s under a load of 15 N is shown in Fig. 5.38. The untreated SREC's worn surface was marked by significant fiber severing and a large amount of fiber and matrix debris (Fig. 5.38(A)). The fibre was almost totally detached from the epoxy matrix, as seen in Fig. 5.38(A), with a considerable fiber-matrix contact gap. The removal of the fibers from the epoxy matrix altered the wear processes from adhesive to abrasive, causing the matrix to micro-cut and furrow faster. The untreated SFREC's' transfer film was dense and irregular, with a substantial amount of transferred wear particles visible on the counterpart surface, indicating the composite's poor wear resistance. Both SAT SFREC and SCT SFREC worn surfaces were smoother, and adhesion and plough marks were less severe when compared to UT SFREC (Fig. 5.38(B,C)). The sisal fibers are well bound to the epoxy matrix, indicating that the surface treatment of

the fibers helps to successfully boost the interfacial bonding strength between the fibre and the resin, hence greatly improving the composite's tribological capabilities. The transfer film of the SCT SFREC became comparably thinner and more homogeneous, conforming to the composite's best wear resistance.

5.3.4 Effect of operating parameters and chemical modification on tribological properties of JFREC

5.3.4.1 Specific wear rate (SWR)

SWR of untreated and treated JFREC are plotted against varying normal loads (10 N, 15 N, 20 N, and 25 N) in Figure 5.39 at a constant sliding velocity of 1.8 m/s to analyse the impact of normal load on the wear volume loss of the composites. From the Fig. 5.39(A), it is evident that as the applied load increases, the SWR also increases for all the tested composite specimens. Similar observation can also be found in several literature [126,127]. This may be attributed to the high heat produced at the interface, contributing to the epoxy matrix being softened, resulting in increased material removal of the composites [128]. Fig. 5.39(A) revealed that the lowest SWR is acquired for sodium carbonate treated (ST) JFREC is 0.0061 mm^3/Nm at 10 N applied load and the highest SWR is acquired for untreated JFREC is 0.0244 mm^3/Nm at 25 N applied load.

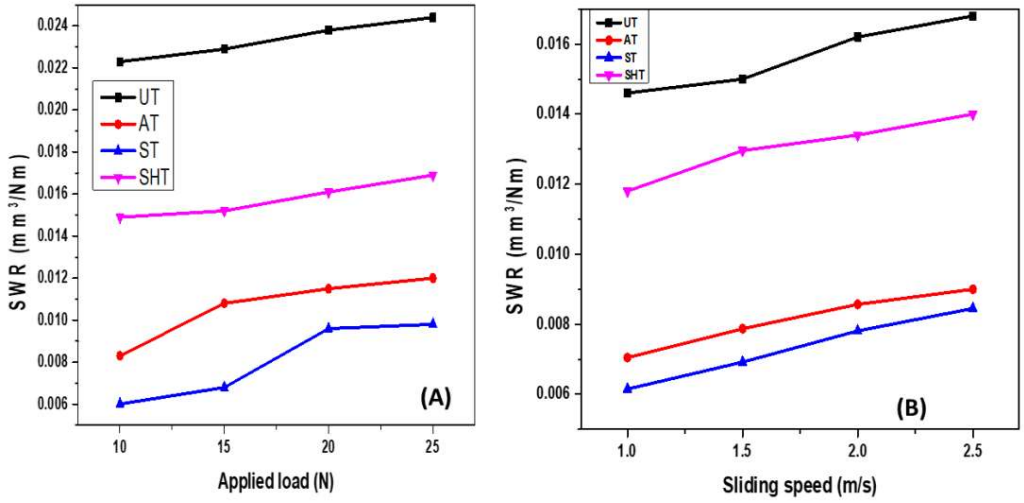

Figure 5.39 Tribological properties of JFREC (A) SWR vs Applied load and (B) SWR vs Sliding speed

SWR of untreated and treated JFREC are plotted against varying sliding velocities (1 m/s, 1.5 m/s, 2 m/s, and 2.5 m/s) in Fig. 5.39(B) at a constant applied load of 20 N to analyse the impact of sliding velocity on the SWR of the composites. From the Fig. 5.39(B), it can be visible that as the sliding velocity increases, SWR of JFREC also increases. Increase in sliding velocity results in greater frictional heat production and this heat triggered the epoxy's mechanical properties to degrade and the polymer's wear resistance to decrease [51]. This may be the reason for increased SWR with increase in sliding speed. Fig. 5.39 revealed that the lowest SWR is acquired for sodium carbonate treated JFREC is 0.0057 mm^3/Nm at 1 m/s sliding speed and the highest SWR is acquired for untreated JFREC is 0.0168 mm^3/Nm at 2.5 m/s sliding speed. From Fig. 5.39(A,B), it is also observed that under identical wear test conditions, chemically treated JFREC depicted less SWR relative to untreated JFREC. Treatments with sodium hydroxide, sodium carbonate and sodium hydrogen carbonate helped loosen the exterior part of the fiber and made it rougher as the fibrils

increased. This leads to an improvement in the fibers' interaction areas with the matrix, promoting stronger mechanical interlocking connecting the jute fibre and the epoxy matrix [51,56,126]. The explanations set out above are possible reasons for the lower SWR values of the treated JFREC. From Fig. 5.39(A,B), it is also observed that the ST JFREC showed the maximum wear resistance, followed by AT JFREC, SHT JFREC and UT JFREC.

5.3.4.2 Coefficient of friction

Fig. 5.40 presents a typical curve for the composites' coefficient of friction (COF) as a function of time. The COF vs. time curves for the UT JFREC, AT JFREC, ST JFREC and SHT JFREC are displayed in Fig. 5.40. The results show that the COF values fall between 0.5 and 0.3. These numbers are in the same ballpark as those for dry sliding wear in other composites of polymer resin reinforced with additional natural fibres [131-132] or glass fibres [133-134] employing a steel counter-body. This might imply that the resin is primarily responsible for the composite's coefficient of friction on steel, with fibre playing a minor role. The results shown in Fig. 5.40 demonstrate that the behaviour of the COF is stable for all substances tested within the range of the tribological test, with no significant variations in the curves. This might imply that the system is not experiencing a significant stick and slip process. Nonetheless, fluctuating behaviour in the HFREC has been seen in the literature [132-133] and might be regarded as usual. According to Viáfara and Sinatora [135], this oscillating phenomena might be caused by adhesion in the asperities of the contacting surfaces.

Coefficient of friction (COF) of untreated and treated JFREC are plotted against varying normal loads (10 N, 15 N, 20 N, and 25 N) in Fig. 5.41(A) at a constant sliding velocity of 1.8 m/s to analyse the impact of normal load on the COF of the

composites. From the Fig. 5.41(A), it can be seen that as the applied load increases, the COF also increases for all the tested composite specimens. If the applied load is increased, the contact pressure between the steel ball and the composite specimen also increases, which led to an enhancement in the interface temperature, that, in fact, results in a rise in friction force [128]. This may be the explanation for the enhancement in COF at higher loads. Fig. 5.41(A) indicates that the maximum COF is obtained for untreated JFREC is 0.56 at a load of 25 N and the minimum COF is obtained for ST JFREC is 0.352 at a load of 10 N.

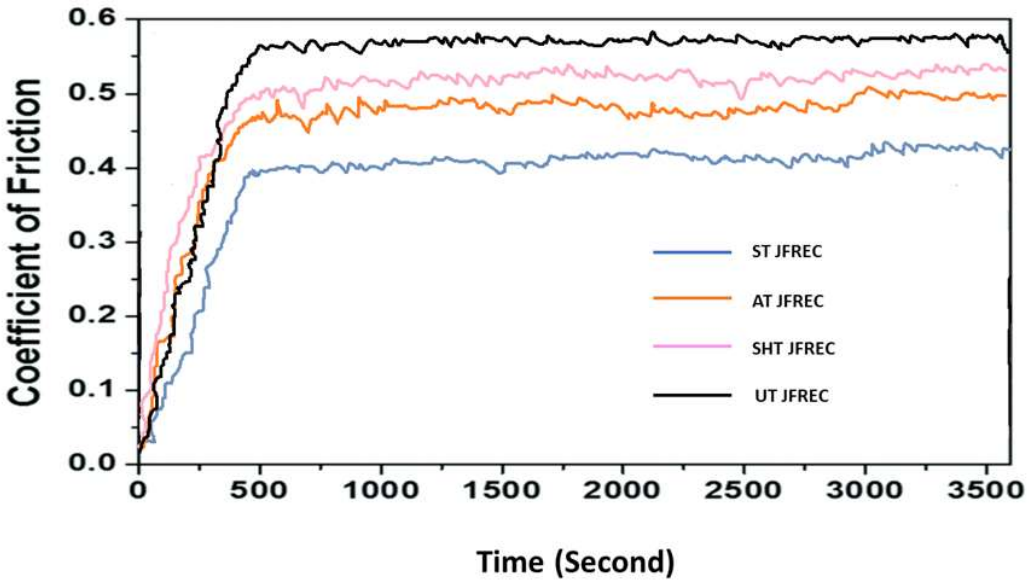

Figure 5.40 COF Vs Time graph for chemically treated JFREC

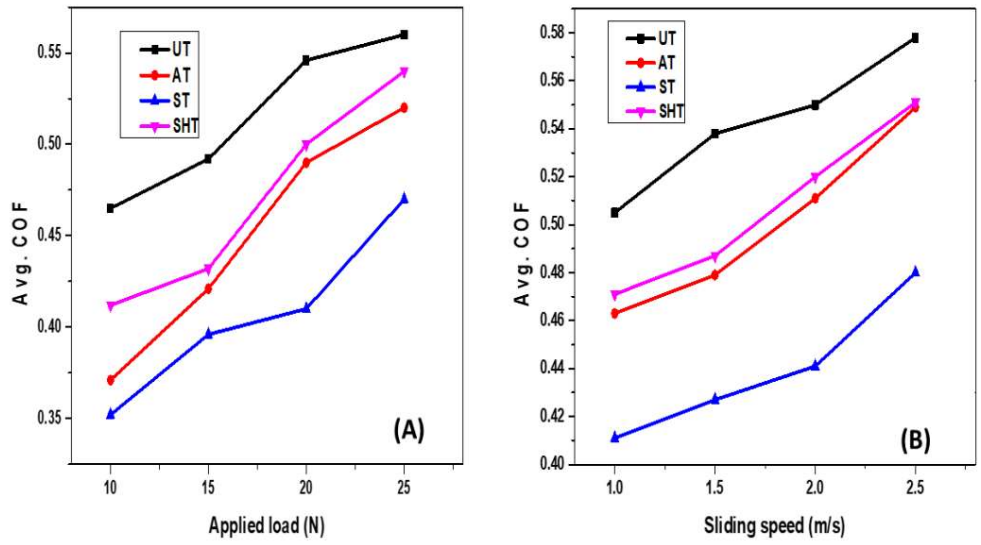

Figure 5.41 Tribological properties of JFREC (A) Avg. COF vs Applied load and (B) Avg. COF vs sliding speed

COF of untreated and treated JFREC are plotted against varying sliding velocities (1 m/s, 1.5 m/s, 2 m/s, and 2.5 m/s) in Fig. 5.41(B) at a constant applied load of 20 N to analyse the impact of sliding velocity on the COF of the composites. From the Fig. 5.41(B), it can be seen that as the sliding velocity increases, the COF also increases for all the tested composite specimens. The heat is produced at the interface between the specimen and the steel ball as the composite specimen rotates at a certain velocity. If the sliding velocity increases, it also increases the amount of heat produced, which enhances the interface temperature, which in turn increases the frictional force [119]. This may be the explanation for the enhancement in COF values at higher sliding speeds. From Fig. 5.41(A,B), it is also observed that under identical wear test conditions, chemically treated JFREC depicted less COF relative to untreated JFREC. The surface viscosity of the material decreased, mostly due to the strong bond between the treated fibre and the matrix. This led to the development of a lubricant

layer that prevent the deprivation of material and reduced the COF [126,128]. Fig. 5.41(B) indicates that the highest COF is obtained for untreated JFREC is 0.57 at a sliding speed of 2.5 m/s and the lowest COF is obtained for ST JFREC is 0.41 at a sliding speed of 1 m/s. From the Fig. 5.41(A,B), it is also observed that the ST JFREC has the most desired COF values (0.3-0.5) for break pads followed by AT JFREC, SHT JFREC, and UT JFREC.

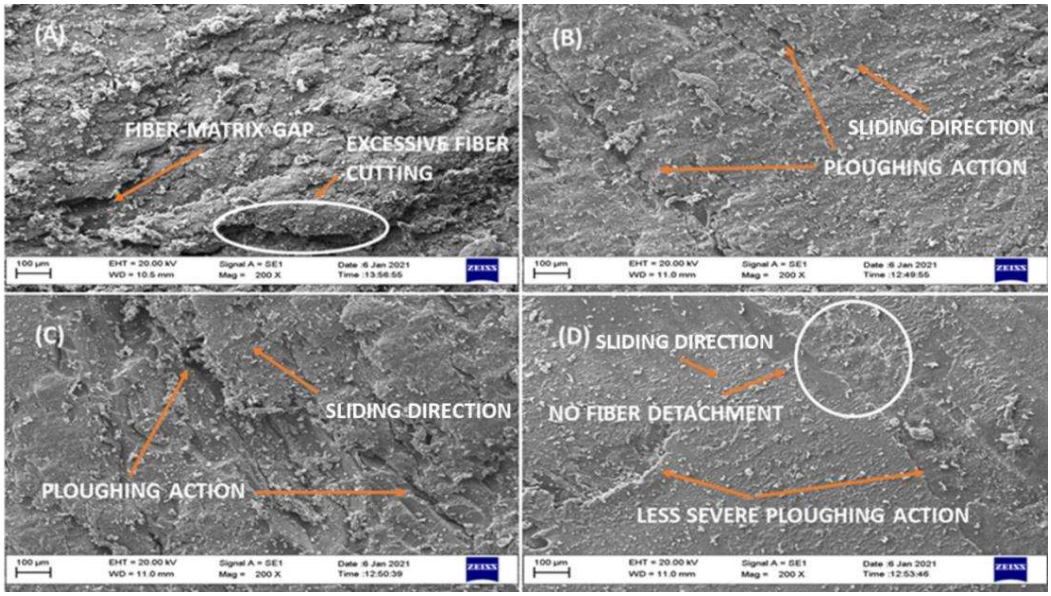

Figure 5.42 SEM images of worn surfaces of JFREC at 20 N load and 2 m/s sliding speed: (a) UT JFREC (b) AT JFREC (c) ST JFREC and (d) SHT JFREC.

5.3.4.3 SEM micrographs of worn surfaces of composites

Fig. 5.42 shows the SEM images of the worn surface of UT JFREC, AT JFREC, ST JFREC, and SHT JFREC against a steel ball at 20 N normal load and 2 m/s sliding velocity. Extreme fibre cutting and plenty of wear debris from fibers and epoxy matrix defined the worn surface of the untreated JFREC (Fig. 5.42(A)). From the Fig. 5.42(A), it is also observed that the jute fibers were almost entirely isolated from the

epoxy matrix, with a substantially wide fiber-matrix interface gap. The pull out of the jute fiber from the epoxy matrix may have changed the wear process from adhesive to abrasive [56]. The transfer film of the untreated JFREC was dense and irregular; on the counterpart (steel ball) surface, a significant volume of transferred wear debris was found, which resonated to the untreated JFREC's low wear resistance [130].

The worn surface of AT JFREC, ST JFREC, and SHT JFREC was smoother, and the plough and adhesion spots are less visible in comparison to untreated JFREC (Fig. 5.42(B,C,D). From the Fig. (5.42(B,C,D)), it is also observed that the jute fibers are well attached to the epoxy, which means that the jute fiber surface treatments leads to the enhancement of the interfacial strength between the jute fibre and the epoxy resin and thereby substantially increase the treated JFREC's tribological properties. Fig. 5.42(C) indicates that the transfer film of ST JFREC has been relatively uniform, acknowledging the superior wear performance of the ST JFREC. Fig. 5.42(A) revealed that on the worn surface of the untreated jute fiber/epoxy composite, the wear debris were adhered to the surface and moderately deformation flow occurred. This suggested that adhesion was the key wear mechanism for untreated JFREC. However, ploughing was the dominant feature on the worn surface of treated JFREC .

Chapter summary

The following topics are discussed in this chapter:

- The results and discussions of water accumulation, mechanical and tribological characterization of NFRECs employed for the evaluation of fiber-matrix mechanical interlocking connecting the natural fibers and polymer resin.

The conclusions derived from the experimental results will be discussed in the next and the final chapter of this thesis.